TECHNISCHE UNIVERSITÄT
ILMENAU

Faculty of Electrical Engineering and Information
Technology Institute for Media Technology
Audio Visual Technology

Master Thesis

Enhancing Drone Operations within the Industrial Metaverse

Submitted by: Qasim Saboor

Major: Media Technology

Professor: Prof. Dr.-Ing. Alexander Raake
Advisor: Dr.-Ing. Stephanie Arévalo Arboleda

Ilmenau, 23rd August 2024

ACKNOLEDGEMENTS

I would like to express my sincere gratitude to Prof. Dr.-Ing. Alexander Raake for providing me with the opportunity to work on this master's thesis and for allowing me to be part of his esteemed department. His guidance and suggestions were instrumental in the completion of this thesis. I am deeply appreciative of his continuous support and valuable feedback throughout this journey.

I also wish to extend my deep gratitude to Dr.-Ing. Stephanie Arévalo Arboleda for her exceptional supervision. It has been a pleasure working under her direction. Her excellent monitoring, guidance, and deep subject knowledge have been invaluable to the accomplishment of my thesis work.

I would also like to thank all members of the Audio-Visual Technology department for their constructive feedback and support. Their contributions have significantly enriched my research experience.

Finally, I would like to express my heartfelt thanks to my family and friends for their unwavering support and encouragement throughout my master's studies. Their belief in me has been a constant source of motivation.

ABSTRACT

The increasing integration of drones into various industrial applications has underscored the need for optimizing their operational efficiency and task performance. One critical aspect of drone operation is the camera angle, which significantly influences the operator's situational awareness, cognitive load, and overall task effectiveness. This thesis explores the impact of different camera angles of drone inside a factory environment on task performance, situation awareness and workload in two specific operations: assembly line monitoring and drone delivery. Understanding the optimal camera angle can enhance error detection, reduce mental and physical strain on operators, and improve task execution efficiency. This thesis systematically evaluated the effects of three camera angles 0°, 45°, and 90° on task performance, situational awareness, and workload. Using a Virtual Reality (VR) factory environment to simulate real-world conditions, participants were tasked with identifying errors in an assembly line and executing a drone delivery task. The study revealed that the 45° camera angle consistently provided the best performance in the assembly line monitoring task, resulting in the shortest total time and the highest number of errors detected. Conversely, the 90° camera angle excelled in the drone delivery task, demonstrating the lowest total completion time and the highest precision in navigation. The situational awareness assessments indicated that the 90° angle offered lower instability and complexity in the assembly line task, while the workload evaluations showed that the 45° angle minimized physical and mental demands. The findings of this research highlight the importance of selecting appropriate camera angles based on specific task requirements. These insights can guide the development of more effective drone operation protocols, ultimately improving industrial productivity and operator well-being.

1 Table of Contents

1 Introduction

The evolution of Industry 4.0 brings together a suite of integrated technologies that have the potential to revolutionize the manufacturing industry. Notable examples being part of this revolution are the Internet of Things (IoT), Digital Twins (DT), Cloud Computing, and Virtual Reality Simulations (VRSIM) [1]. Industrial drones, which are in high demand among various industries, when combined with these technologies can be of various benefits. Industries are increasingly adopting drones to perform a wide range of tasks, including transportation of materials from storage to the manufacturing floor and moving finished products from production to shipment, significantly reducing labor costs. A major use case is the telecom industry; drones are frequently utilized to conduct site audits quickly and efficiently, promptly providing top-down views and line-of-sight inspections [2]. Not only this, drones can also scan transmission lines, inspect boilers, monitor solar panels, assess storm damage, and perform repairs more quickly than humans. This technology serves as a cost-effective and more efficient alternative to helicopter-based operations, reducing both acquisition and maintenance expenses. Additionally, drones facilitate AI-driven data analysis to enhance the precision of their monitoring systems [3][4]. Their easy deployment enhances site security and safety during inspections [5][6]. Drones enable better maintenance planning, asset monitoring, and fault investigation through regular and consistent data collection. Contributing significantly to Industry 4.0, drones drive companies to push technological innovation to the next level.

Drones, or unmanned aerial vehicles (UAVs), have swiftly become essential tools in the manufacturing sector. Equipped with advanced technologies like high-resolution cameras, thermal imaging sensors, and Artificial Intelligence (AI) capabilities, these drones are transforming manufacturing operations [7]. Their integration into industrial processes is driven by the need for efficiency and cost-saving measures, helping businesses remain competitive. By swiftly inspecting hard-to-reach areas, drones can detect potential issues or hazards before they escalate into significant problems, thereby enhancing the overall efficiency of manufacturing facilities [8]. Furthermore, drones offer a safer alternative for workers compared to traditional inspection methods, which are often hazardous and time-consuming. Employing drone technology minimizes workplace accidents, boosts overall safety, and enhances productivity. The data collected by drones enable manufacturers to make informed decisions regarding resource allocation and optimize the manufacturing process. This shift not only improves operational efficiency but also reinforces safety measures within the industry [9].

One of the most promising uses of drones in infrastructure is factory surveillance and maintenance. Drones equipped with high-resolution cameras and sensors monitor machinery and detect issues

before they become major problems, saving time and money on repairs and reducing facility downtime [10]. These drones can access hard-to-reach or dangerous areas, providing real-time inspections without disrupting operations and ensuring worker safety. Additionally, drones enable remote inspection capabilities, allowing off-site experts to analyze live video streams and advise on necessary repairs or adjustments. This integration of drones into factory operations significantly improves efficiency, reduces costs, and enhances safety measures, making them a transformative technology for the manufacturing industry.

2 Related Work

Awasthi et al. conducted a study on the safety and feasibility of using a swarm of UAVs indoors alongside humans, aiming to demonstrate that it is both feasible and safe to integrate UAV swarms into indoor environments under the industry 4.0 framework [12]. While UAV swarms have primarily been used in outdoor civil and military applications, the study highlights their potential for enhancing manufacturing and supply chain management by improving data collection, monitoring, and decision-making within an IoT framework, and automating redundant tasks. The study concludes that UAV swarms can safely automate various industrial tasks, with future plans to use larger UAVs for actual packages and integrate recharging stations, as well as improve indoor localization techniques to reduce dependence on expensive motion capture systems. This study by Awasthi et al. is relevant to our research on the impact of different drone camera angles on task performance, situational awareness, and workload in industrial settings. Both studies focus on enhancing the practical use of UAVs in industrial environments and highlight the potential for UAVs to optimize various tasks and improve efficiency. While Awasthi et al. explored the feasibility and safety of using UAV swarms for package transportation indoors, our study is also focused on the delivery of packages inside the factory using the drone. Both studies underscore the importance of integrating UAV technology into industrial operations to enhance productivity and reduce human workload. The study by Mourtzis et al. investigates the limitations of integrating UAVs into modern manufacturing systems and proposes an intelligent path-planning algorithm based on the A* algorithm in three dimensions to address these limitations [11]. Their research highlights the ongoing challenges and opportunities for further investigation into the effective integration of drones. They emphasize that suitable frameworks can affect the physical load on human operators and provide production engineers with advanced remote monitoring tools, thereby enhancing productivity. The study predicts that reducing shop-floor technicians' traveling distance could decrease their fatigue by 10% to 20%, depending on the job type and shop-floor size, and improve overall manufacturing productivity by about 3%. The research also stresses the necessity of establishing safety regulations and operation protocols to ensure human safety in collaborative environments with drones. Their proposed framework incorporates distance limitations to avoid collisions, excluding cells lower than 2 meters from the grid to ensure safety. This study by Mourtzis et al. is related to our research on the impact of different drone camera angles in a factory environment and how it can optimize task performance. While Mourtzis et al. focused on path-planning algorithms and physical load reduction, our study examined how specific camera angles influence performance metrics, situation awareness and workload during drone operations.

Maghazei et. al implemented virtual simulation and discusses how such simulations can inform the use of automatic drones for factory inspection. Automatic drones can improve indoor manufacturing processes, particularly repetitive tasks such as inspection operations, intralogistics for small parts, cycle counting in warehouses, security monitoring, ergonomic monitoring, risk monitoring, and building information modeling [13]. Implementing automatic drones involves considerable technological and operational challenges. This research showed that virtual simulations can animate automatic drone flights in 3D and help better understand the technological and operational challenges of using new technologies in real manufacturing environments and support decision-making and problem-solving processes. For instance, factory planners can use simulation models to evaluate, allocate, and design airspace for drone flights. Virtual simulation of automatic drones also helps set and define safe flight zones for indoor airspace, which helps quickly evaluate various scenarios, such as trade-offs between coverage, speed, and risks. Furthermore, factory managers can use 3D models to communicate and collaborate with drone technology developers, as well as sensor manufacturers and robotics companies, by virtually presenting the technological requirements of using automatic drones with embedded sensors/technologies in their settings. For instance, primary metal companies would require drones and thermal cameras that can cope with high temperatures, petrochemical companies require explosionproof drone systems, and e-commerce warehouses may benefit from collaborative drone technologies (i.e., swarming) with advanced path planning and fleet management systems. Zenkin et al. conducted a simulation study of drones designed to monitor large areas, considering scenarios such as detecting fire sources in forests, intruders in restricted territories, and their vehicles [14]. The study results showed that higher altitudes allowed faster area coverage but reduced detection accuracy due to smaller object sizes and increased localization errors. They also noted that the fire recognition algorithm performed consistently across various altitudes and speeds due to its reliance on the fire's color palette. This study by Zenkin et al. is relevant to our research on the impact of different drone perspectives on task performance, situational awareness, and workload in monitoring. Both studies underscore the importance of visual perspectives in optimizing drone operations. While Zenkin et al. emphasized altitude's role in balancing area coverage and detection accuracy, this thesis highlights how specific camera angles influence performance metrics, situational awareness, and workload during drone operations. Both studies reveal that optimal visual configurations whether through altitude or camera angles are crucial for enhancing efficiency and accuracy in drone operations.

Oh et al. developed a prototype connecting Virtual Reality and Mixed Reality to provide both first-person and third-person views for pilot training, focusing on flight situation monitoring and debriefing [15]. The study involved six flight instructors who assessed the third-person view situations using a

HoloLens headset. While the system did not show obvious effectiveness over conventional first-person VR simulations or VR simulations with a 2D debriefing map, instructors with fewer than 1,000 flight hours noted the potential benefits of the third person view for identifying pilots' weaknesses during debriefing. The prototype's flexibility in offering both views was appreciated, indicating its potential for better flight debriefing. However, instructors with more than 1,000 flight hours, who are more accustomed to traditional debriefing methods, were less receptive due to the prototype's functional shortcomings, such as time synchronization issues and visualization delays in the MR application. This research by Oh et al. is relevant to our study on the impact of different drone view perspectives in drone operations. Both studies explore innovative applications of VR technologies to enhance training and operational efficiency. While Oh et al. focus on pilot training by integrating VR and MR to provide diverse perspectives during flight debriefing, this thesis examines how different drone camera angles affect performance, situational awareness and workload in industrial operations.

This thesis includes three camera angles: 0°, 45°, and 90°. These angles were chosen based on insights from previous research [23], which highlighted their effectiveness in various visual and detection tasks. The 0° angle faces forward in the direction of the drone, providing a perspective similar to a human's line of sight and is useful for tasks requiring forward navigation and obstacle avoidance. The 45° angle is inclined, offering a balanced view that combines both forward and downward perspectives, making it ideal for monitoring and identifying objects with spatial context. The 90° angle faces directly downward, maximizing the field of view for tasks involving surface inspection and detailed examination of areas directly beneath the drone.

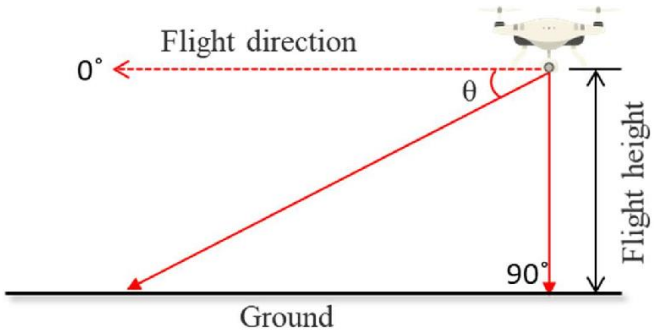

Figure 1. Drone Camera Angles

To enhance user experience and minimize motion sickness during the simulation, a camera lens-like object was strategically attached to the bottom surface of the drone, with the VR origin placed inside this lens to achieve a specific, consistent camera angle and limit the user's field of view. This method was chosen as it aligns with the previous researches [24][25][26]. The camera lens object was designed to be open only at the front, providing a clear view of the environment while the sides and back

remained blacked out. This configuration helps narrow the user's field of vision, reducing peripheral distractions and motion inconsistencies, which are common causes of motion sickness in VR applications [27]. By bounding the user's view to a specific angle, the lens setup ensures that the user can only see the environment through the designated front opening, aiding in maintaining spatial orientation and reducing the sensory overload that can occur with a wider, unrestricted view. Positioning the VR origin within the camera lens helps create a stable and immersive viewpoint, aligning the user's perspective with the drone's movement. This alignment is crucial for providing a realistic and comfortable VR experience, as it synchronizes the visual and physical sensations of motion. To further enhance user comfort and accuracy, a reset position feature was integrated. The right controller's trigger button was bound to reset the user's position to the center of the lens, allowing users to re-center their view at any time and ensuring they can always achieve an optimal and consistent perspective. This feature also helps maintain the accuracy of specific camera angles critical for tasks like assembly line monitoring and package delivery. The reset position functionality is particularly beneficial as it allows users to perform tasks regardless of their physical posture—whether sitting, standing, or moving around. No matter the user’s initial position, the reset feature realigns their view to the center of the lens, facilitating a consistent and comfortable viewpoint. This ensures that the user's perspective remains stable and correctly aligned with the drone's operations, providing precise visual data for task performance and evaluation. The lens design and reset functionality work together to reduce the likelihood of motion sickness. By limiting the field of view and providing a stable, centered perspective, users experience fewer visual inconsistencies, which are a primary cause of VR-induced discomfort. This setup ensures that the user's viewpoint is consistently aligned with the intended camera angles, providing precise visual data for task performance and evaluation. The ability to reset the position on demand gives users control over their viewing experience, enhancing comfort and reducing fatigue during extended use. The constrained field of view focuses the user's attention on specific tasks and reduces distractions, improving task efficiency and accuracy.

3 Implementation

3.1 Hardware

- Meta Quest 3.0

Figure 2. Meta Quest 3.0

- D-Link VR Air Bridge

Figure 3. D-Link VR Air Bridge

3.2 Softwares

- Unity 3D v2022.3.15f1
- Meta Quest Link App v66.0.0.308.370
- Blender 4.1
- Autodesk 3ds Max v2025
- Nvidia Omniverse v1.9.11
- Visual Studio Community v2022
- Anaconda v2024.02-1
- Jupyter Notebook v7.0.8
- RStudio v2024.04.2-764

3.3 Programming Languages

- C#
- Python

3.4 Prototype

3.4.1 Environment Creation

The virtual environment was created inside Unity 3d [16] manually without any auto terrain tool by using different assets from the Unity Asset Store [17], TurboSquid [18] and GrabCAD [19] and some of the assets were modified later according to the requirement of the environment using Blender [20], 3ds Max [21] and Omniverse [22]. Factory components such as robotic arms, conveyor belts, shifters, rotating tables, rims, tires, cars, pallets, drones, shutters, workstations, lights were added to give it a complete factory look. To enhance the ambience, particle systems were introduced to simulate the spark effect from the robotic arms' heads. Post process layer is used to enhance the visuals by customizing post processing effects such as bloom, vignette, chromatic aberration, depth of field, film grain, tone mapping and white balance. Additionally, auditory cues were added to complete the immersive factory experience.

Figure 4. Factory Environment

3.4.2 Simulations and Animations

All the animations were created manually in Unity 3D and Blender to ensure a high level of detail and accuracy in simulating the tire assembly process. Animation blending techniques were employed to create smooth transitions between different animation states, enhancing the realism of robotic movements. Animation events were strategically used to trigger specific scripts and interactions at precise moments, replicating real-life factory operations. These events allowed for the synchronization of various components and actions within the simulation, such as the switching of robotic tool heads and the initiation of quality tests. By combining these detailed animations with realistic movement and timing, the virtual environment effectively mimics the intricate workflows of an actual tire assembly line, providing an immersive experience.

The assembly line for car wheels manufacturing consists of multiple workstations. In each workstation, there are two robotic arms: one large and one small. The larger arm first tests the rims, which are placed on the rotating table one by one, making them rotate and warm up to ensure material integrity. It then grabs the rubber tires and precisely aligns them with the rims before placing them. The arm then applies pressure to fix the rubber onto the rims securely. Once the rubber is fixed, the robotic arm switches its tool head to a gripper and transfers the assembled tire to a testing machine. This machine performs various tests, such as balance and durability, by rotating the tire and applying simulated road conditions. After testing, the larger robotic arm retrieves the tire and places it in the ready station. The smaller robotic arm then conducts a final quality inspection on the tire to check for

any defects or imbalances. After confirming the tire meets all quality standards, the arm switches its tool head to a gripper, picks up the tire, and places it onto the conveyor belt for the next stage of assembly.

On the subsequent assembly lines, the process of attaching tires to cars is replicated as happens in real factories. Two robotic arms work parallel for each car that passes by. Initially, the front tires are handled. The robotic arms precisely position the tires onto the car's wheel hubs using advanced sensors and alignment tools. Once the tires are in place, the robots switch their tool heads to bolt-tightening mechanisms, securing the tires with the correct torque to ensure safety and performance standards. The conveyor belt, designed to carry cars at a controlled speed, then moves the car forward to the next station where the rear tires are attached. The process is identical to the front tire attachment: the robotic arms position, align, and secure the tires with precision.

Animation events trigger specific scripts and interactions at precise intervals, replicating the real-life timing and coordination found in actual factories. This simulation not only visualizes the sequence of operations but also allows for testing and optimization of workflows, ensuring an accurate and efficient tire assembly process in the virtual environment. To enhance the realism, the virtual environment also includes auditory cues, such as the sounds of machinery and robotic movements, and visual effects like sparks from welding and lighting variations to mimic factory conditions. These effects are manually created using shaders and particle system in Unity 3d. This comprehensive simulation provides a detailed and immersive representation of the tire assembly process, mirroring the complexities and precision of real-world manufacturing.

Figure 5. Assembly Line

3.4.3 Way Points

Waypoints were implemented for the precise movement and navigation of the drone within the virtual factory environment. Waypoints are predetermined locations that serve as key navigation points for the drone, guiding it along a specified path. Each waypoint is strategically placed to ensure optimal coverage and efficiency in the drone's tasks, whether it's for monitoring the assembly line or performing delivery functions. Waypoints were implemented to restrict user movement to specific locations within the virtual environment, ensuring they only navigate to predetermined points. This approach not only saves time during the study but also ensures the accuracy of the results by standardizing the participant's path. Participants can move forward or backward along the waypoints, allowing for a controlled and consistent navigation experience. By limiting movement to these predefined paths, we can better focus on the study's objectives and gather precise data on how different camera angles affect situation awareness, task performance, and workload.

3.4.4 Drone Control

The drone control system was designed to streamline user interaction and ensure precise movement for accurate data collection. The controls were mapped to the right and left controllers of Meta Quest 3. For the right controller, A and B buttons were bound to move the drone forward and backward, respectively. Pressing the B button propels the drone forward, while the A button moves it backward. The grip button was utilized to select errors in the assembly line using a ray cast. This ray cast feature enabled users to identify and select errors present at various stations. The trigger button was bound

to reset the drone's position to the center of its camera lens, allowing for easy reorientation. For the left controller, Y and X buttons were bound to control the drone's altitude. Pressing the Y button raises the drone, while the X button lowers it.

Figure 6. Drone Controls

3.4.5 Task Design

In the prototype, two drone tasks were implemented in the factory environment, assembly line monitoring task and drone delivery task.

3.4.5.1 Drone Assembly Line Monitoring Task

In the drone assembly line monitoring task, the drone's movement was limited to forward and backward direction. The primary objective in this task was to identify and select errors on the assembly line. A ray cast was implemented on the right-hand controller to facilitate error detection. When user directed the ray cast at an error and pressed the grip button on the right controller, the error would be selected and marked as resolved. On selecting the error, a sound "error detected" will be initiated confirming the selection of the error. Errors were visually indicated with a red light, which disappeared once detected and selected by the user. This method ensured precise and efficient error identification, providing clear feedback to the user.

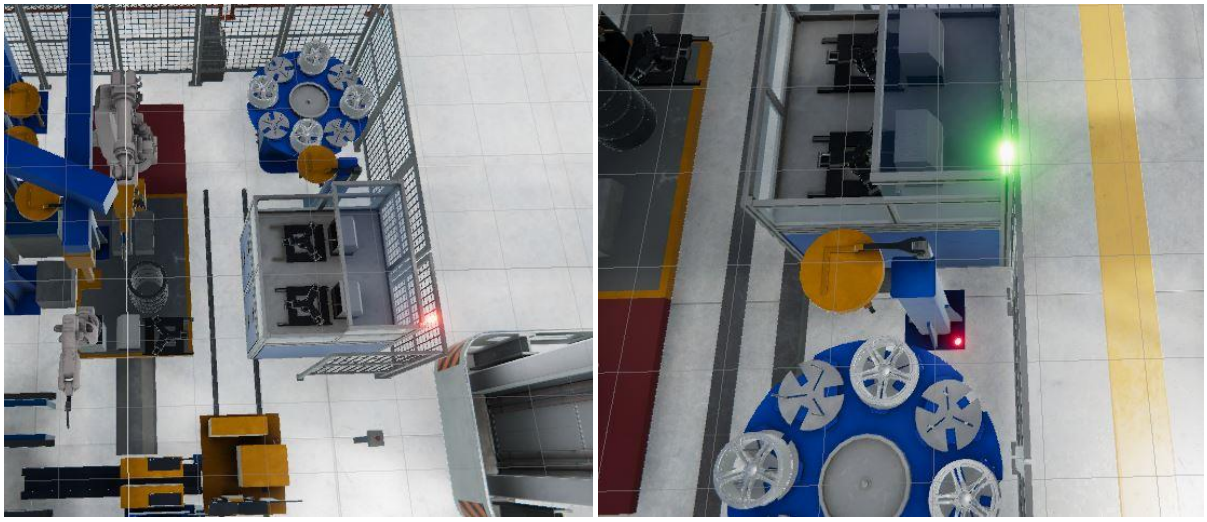

Figure 7. Red light indicating errors on assembly line

3.4.5.2 Drone Delivery Task

The drone delivery task required the drone to transport a package from the pick-up location to a designated drop-off area. In this task, the drone's movement was limited to forward, backward, upward and downward direction. Different shader effects were implemented to direct the drop-off area. Upon reaching the pick-up area, the drone had to land precisely on top of the package to initiate the collection process. When the drone successfully landed on top of the package, a sound "item picked" will be initiated to confirm that package is successfully picked. Once the package was secured, the drone could ascend to the maximum height before moving forward to the drop-off area. Upon arrival, the drone would descend to the minimum height to place the package accurately in the drop-off zone. When the drone drops the package in the drop-off zone, a sound "item dropped" will be initiated to confirm that the package is successfully dropped.

Figure 8. Pick up and drop off stations for drone delivery

In both tasks, the drone simulation starts from a specific height and drone take off was not considered. Drone must achieve a maximum height of 15 meters to move forward. The minimum height which drone can achieve is 1.4 meters. A maximum height of 15 meters was chosen to bring the entire assembly line into the drone's field of view, ensuring accurate results. The minimum height of 1.4 meters was necessary for the drone to grab packages from conveyer belt, as this is the height required to reach the package placed on top of the conveyer belt. In assembly line monitoring task, drone cannot move in downward direction but for drone delivery task, the drone can move downward to collect and drop the package. This restriction was implemented to ensure consistent navigation and prevent premature forward movement, which could affect task accuracy and data collection. During the drone delivery task, the weight of the package which the drone picked up remained constant and had no effect on drone flight, further standardizing the experiment. A cylindrical camera lens was attached to the drone, with participants virtually positioned at its center, narrowing their field of view to a stable angle that moved with the drone. The camera angles were adjusted using a ring-based method used in previous research [24][25][26][27], allowing fixed angles of 0°, 45°, and 90°. The lens was designed with black sides and a black backside to restrict visibility to only the front, ensuring participants always faced forward, thus maintaining a consistent visual field. The speed of the drone was maintained constant at 5 meters per second to ensure stable and accurate da

3.4.6 Timer

To ensure precise measurement of task performance, a comprehensive timer system was implemented in the prototype. This system calculates time in minutes, seconds, and milliseconds, and is designed to provide accurate data for analyzing user performance across different tasks. The timer system gets activated when the drone enters the maximum height for the first time. This ensures that the timing data accurately reflects the operational phase of the tasks, eliminating any inconsistencies that could arise from the drone's initial setup and ascent.

Three distinct timers were implemented to capture various aspects of the tasks. The first timer, total task time, records the total duration from the start line, located at the beginning of the assembly line, to the finish line at the end. It begins when the drone reaches its maximum height of 13 meters for the first time and stops when the drone enters the finish line, providing a comprehensive measure of the overall task duration and capturing all phases of the drone's operation. This timer is used in both tasks. The second timer was implemented to record time taken to pick-up the package, it starts when the drone enters the start line and stops when the drone successfully reaches and lands on top of the package. This metric is crucial for understanding the efficiency of the drone's navigation and approach phase and is used only in the drone delivery task. The third timer, time taken to drop-off the package,

calculates the duration from the successful pick-up to the package drop-off. It begins once the drone secures the package and stops when the package is placed in the drop-off zone, helping analyze the efficiency of the drone's transport and delivery phase. This timer is only used in drone delivery task.

3.4.7 Error Detection

For error detection, a ray cast mechanism was implemented, exclusively activated during the drone assembly line monitoring task. The error detection system operates solely within this task. Users direct the ray cast at errors, which are indicated by red lights randomly distributed across the stations. By pressing the grip button on the right controller, the user can select an error. Upon selection, the red light disappears, and the error count is incremented. This process continues for each subsequent error, incrementing the count with each detection. Errors can be located on any machine within any station of the assembly line. The error detection system is activated when the drone crosses the start line and deactivates when the drone reaches the finish line, at which point the final error count is displayed. To ensure accurate data, the drone is maintained at a constant maximum height throughout this task, providing a stable perspective for precise error identification.

3.4.8 Distance to Target

Distance measurement was implemented to evaluate the precision of the package drop-off in the drone delivery task. This feature calculates the distance between the predefined drop-off target position and the actual position where the user places the package. Upon dropping off the package, the system measures the Euclidean distance between the target coordinates and the coordinates of the package's final position. This measurement process is triggered when the package is released by the user. The last updated distance measurement is displayed once the package is dropped off, providing real-time feedback on the accuracy of the drop-off.

3.4.9 Data Storage

All the collected data, including the timers for total task time for both the assembly line monitoring and delivery tasks, time to pick up the package, time from pickup to drop-off, distance to the target drop-off point, and the number of errors detected, are systematically stored in a CSV file upon the completion of each task. This data logging process ensures that all relevant metrics are accurately recorded for subsequent analysis. The CSV file format was chosen for its simplicity and compatibility with various data analysis tools, allowing for easy export and examination. Each entry in the CSV file includes a timestamp, user ID, and task ID to facilitate the tracking of individual performances across multiple trials. Additionally, the data structure ensures that each metric is clearly labeled, enabling straightforward parsing and interpretation during the data analysis phase.

3.4.10 Auditory Cues

Auditory cues were integrated to enhance the realism and immersion of the virtual environment. Specific sounds were assigned to various factory components, such as robotic arms, welds, rotating tables, stations and testing machines to create an authentic industrial atmosphere. During the tasks, these auditory cues play a crucial role in user interaction and feedback. In the drone delivery task, when the user picks up a package, a distinct “item picked” sound is triggered, providing immediate auditory confirmation of the action. Similarly, upon dropping the package at the designated drop-off point, an “item dropped” sound is activated, reinforcing the completion of the task. For the assembly line monitoring task, auditory feedback is also employed to enhance user experience and task accuracy. When the user identifies an error and presses the grip button on the right controller, an "error detected" sound is emitted. This sound ensures that the error has been successfully registered, reducing any potential confusion and confirming the action for the user. These auditory cues not only contribute to a more immersive and engaging environment but also play a critical role in guiding the user through the tasks and providing essential feedback for successful task execution. Additionally, background ambient sounds were incorporated to simulate the continuous operational noises typical in a real factory setting, such as the hum of machinery and the occasional alert signals. These sounds help in maintaining situational awareness and add to the overall sensory experience. By carefully aligning these auditory elements with visual and interactive components, the simulation achieves a higher level of fidelity and realism, which is essential for accurate training and performance assessment in the industrial metaverse.

3.4.11 Collision Detection

Unity3D’s built-in physics engine is employed to manage and detect collisions. This engine accurately simulates physical interactions between objects, ensuring that the drone responds realistically to its environment. Every object in the environment, including the drone, robotic arms, conveyor belts, and other factory equipment, is equipped with colliders. These are invisible boundaries that define the physical space an object occupies, allowing the physics engine to detect when two objects intersect or come into contact. In addition to colliders, ray casting is used to enhance precision in detecting potential collisions. A ray cast is a virtual line projected from the drone's position in a specific direction. If this line intersects with any object in its path, a collision event is triggered. This technique is particularly useful for tasks requiring high accuracy, such as assembly line monitoring and error detection. Upon detecting a collision, the system executes predefined responses to mitigate any potential issues. For instance, if the drone approaches too closely to a human operator or factory equipment, it can trigger an automatic halt or redirection to avoid contact. This ensures that the drone maintains a safe distance, preventing accidents and ensuring smooth operation. Specific distance

constraints are programmed into the system to further enhance safety. For example, the drone is programmed to maintain a minimum height of 2 meters above the ground and a maximum height of 13 meters. These constraints ensure that the drone operates within a safe vertical range, minimizing the risk of collisions with ground-level equipment or ceiling structures.

4 Evaluation

4.1 Research Questions

To evaluate the impact of different camera angles of drones on task performance, user's situation awareness, and workload, a comprehensive study was conducted. The independent variables in this study were three distinct camera angles: 0°, 45°, and 90°, selected based on previous research. The research questions and proposed hypotheses for this study are outlined as follows:

Research Question: How do different camera angles of the drone affect task performance in terms of time, distance, and errors?

Hypothesis: Different camera angles will have an impact on task performance.

Research Question: How do different camera angles of the drone influence the user's situation awareness?

Hypothesis: Different camera angles will have an impact on the user's situation awareness.

Research Question: How do different camera angles of the drone impact the user's workload?

Hypothesis: Different camera angles will have an impact on the user's workload.

4.2 Participants

A total of 18 participants were recruited for the study with no restriction on age. Among 18 participants 14 were male (mean age of 26.85 years with a *SD* of 0.60) and 4 were female (mean age of 26.25 years with a *SD* of 1.25). Participants who needed vision correction had to wear glasses under the HMD. Among participants whose data was considered only two participants had no experience of VR and sixteen had experience with VR. Similarly, only two participants had experience piloting a drone, whereas sixteen had no prior drone piloting experience.

4.3 Experimental Design

4.3.1 Objective

The objective of this study was to investigate the impact of different drone camera angles on task performance, user's situation awareness, and workload, in drone operations inside a factory environment. The study focused on two specific tasks: the drone delivery task and the drone assembly line monitoring task. The drone delivery task involved picking up a package and dropping it off at a designated area, while the drone assembly line monitoring task required the drone to detect errors along an assembly line.

4.3.2 Independent Variable

The independent variable in the study was the camera angle of the drone. There were three conditions:

Condition 1: Drone tasks with a 0° camera angle.

Condition 2: Drone tasks with a 45° camera angle.

Condition 3: Drone tasks with a 90° camera angle.

4.3.3 Metrics

A total of 3 metrics, which were dependent variables in the experiment, were considered. These dependent variables are:

Task Performance: This includes various sub-metrics such as distance to target measured in meters, total task time, errors detected, time taken to pick up the package, and time taken to drop off the package recorded in seconds and milliseconds.

Situation Awareness: Participants' subjective ratings (Likert scale) of their awareness and understanding of the environment and tasks. Situation Awareness was measured using Situation Awareness Rating Technique (SART) [33].

Workload: Participants' subjective ratings of their perceived workload using the NASA Task Load Index (NASA-RTLX) [32].

4.3.4 Questionnaire Design

A questionnaire was designed to gather participant data, including age, gender, prior VR experience with any head-mounted display (HMD), VR engagement, height phobia, drone experience and susceptibility to motion sickness. For each metric to be measured, questions were sourced from established standard questionnaires and integrated to suit the specific needs of the experiment. Two primary questionnaires were employed: the Raw NASA Task Load Index (NASA-RTLX) [32] and the Situation Awareness Rating Technique (SART) [33]. Participants completed three trials for each camera angle for each task, and after each angle, they were required to fill out both the SART and NASA-RTLX questionnaires. This process was repeated for both the drone delivery task and the drone assembly line monitoring task. The SART questionnaire, with a rating scale from 1 to 7, was used to assess the participants' situation awareness. The NASA-RTLX, with a rating scale from 0 to 20, was utilized to evaluate the participants' perceived workload. In total, participants filled out the questionnaires six times: three times for each task, once after each camera angle. This detailed questionnaire design

ensured the accurate collection of data related to the participants' situational awareness and workload, providing valuable insights into the effects of different camera angles on drone operation performance.

4.3.5 Experimental Setup

The experimental setup utilized the Meta Quest 3 VR headset along with its controllers to navigate the virtual environment. Participants interacted with the environment using these controllers to complete the tasks. Auditory cues were incorporated into the virtual environment through Meta Quest 3's built-in speakers to provide feedback during the tasks. To ensure fairness in the experiment and minimize any potential bias, a Latin square counterbalancing method was employed for both the three camera angles and the sequence in which tasks were performed. This approach divided participants into groups, with each group experiencing the camera angles and task order in a different sequence. This method helps in ensuring that any effects observed are due to the variables being studied rather than the order in which tasks were completed. Using Meta Quest 3 and employing Latin square counterbalancing provided a structured environment to examine how different camera angles and task sequences impact drone operation performance. This setup provided a controlled environment to evaluate user experience, situational awareness, and workload across various experimental conditions.

Figure 9. Experimental Setup

4.3.6 Experimental Procedure

The study was designed with a 60-minute duration, and participants joined voluntarily. Each participant first received a brief overview of the study's purpose, and the hardware devices used, including the Meta Quest 3 headset and controllers. Participants were then asked to sign a consent form agreeing to participate in the study. After obtaining consent, participants were given a comprehensive experiment flow guide document detailing the steps to be followed during the experiment. Hand calibration was performed before proceeding with the experimental tasks to ensure accurate input detection. Participants were trained on the input bindings of the Meta Quest controllers and given a training task to familiarize themselves with drone control and selecting virtual objects using a ray cast. In the training task, they were required to select red balls displayed in the VR headset by aiming the ray at them and pressing the trigger button. Additionally, participants were encouraged to maneuver the drone in all directions such as upward, downward, forward, and backward to gain proficiency in controlling the drone within the virtual environment. After the training session, participants were presented with a comprehensive task document that included all necessary information about the tasks, using both text and images. Depending on the counterbalancing, some participants first completed the drone delivery task while others started with the assembly line monitoring task. In the assembly line monitoring task, participants used a ray cast to select errors indicated by red lights. Upon selecting an error, the light would turn off and a sound cue "error detected" confirmed the selection. Each participant completed three trials for each of the three camera angles (0, 45, and 90°), with the sequence of angles counterbalanced using a Latin square design. The number of errors detected and the total task time for each trial were recorded and stored in an automatically generated CSV file. After completing each angle for each task, participants filled out the NASA-RTLX and Situation Awareness Rating Technique (SART) questionnaires, rating their experience for that specific angle. For the drone delivery task, participants piloted the drone, which could only move forward after reaching a specified maximum height. They were required to pick up a package by landing the drone on top of it, indicated by the sound cue "package picked," and then drop it off at a designated point, confirmed by the sound cue "package dropped." Task performance metrics, including total task time, time to pick up the package, time from pick up to drop off, and distance from the target drop-off point to the actual drop-off location, were recorded and stored in an automatically generated CSV file. Participants followed the Latin square counterbalancing for the sequence of angles in this task as well. An essential aspect of both tasks was the restriction to view through a lens, with the VR origin placed at the center to maintain a specific field of view. The reset position function was bound to the right controller's trigger button, allowing participants to re-center their view manually to reduce motion sickness. Participants were instructed to press the trigger button

if they felt off-center, ensuring consistent data collection for each angle. After completing trials for each angle, participants filled out the questionnaires, resulting in six sets of responses (three for each task). Upon completing both tasks, participants provided feedback on their preferred camera angle, any experiences of dizziness or motion sickness, and general impressions.

Before conducting the main experiment, a significant issue was identified with cybersickness during the testing phase, which occurred when user head movements were limited, and the VR camera was fixed at a specific angle. This discomfort is commonly associated with a disconnect between visual input and physical movement, leading to motion sickness symptoms. To address this problem, a cylindrical camera lens object was attached to the drone. The participants were virtually positioned at the center of this lens, effectively narrowing their field of view to a specific, stable angle that moved with the drone. To validate the effectiveness of this approach, we conducted a pre-test study involving five participants. The results were promising, as none of the participants reported experiencing motion sickness after the cylindrical lens object was introduced. The drone's speed was fixed at 5 units per second, allowing it to move steadily in the direction determined by the button pressed. This speed was selected based on participants feedback in pre-test study, as they reported no motion sickness at this value. These adjustments were crucial in ensuring a smoother and more comfortable VR experience, paving the way for the main experiment to proceed without the disruption of cybersickness.

4.3.7 Analysis Approach

To test the hypothesis for the proposed research questions, qualitative data was gathered into a CSV file using the UniPark tool [28], from questionnaire ratings provided by participants. Data was analyzed using Python programming language in Jupyter Notebook and R. Step-by step analysis was performed in which firstly type of variables was determined if they were categorical, continuous, or ordinal variables. Among the rest of the variables, the Likert scale questions variables were considered ordinal variables. Ordinal variables are often used to measure subjective opinions or attitudes, and they are frequently analyzed using non-parametric statistical tests that do not assume a normal distribution. First, all rating data was converted to numeric form, the overall rating for each participant by averaging across all columns was calculated. After that, from the Python ‘‘Scipy’’ library Friedman test was used for the analysis of data and computation of the p-value. The Friedman test was used because the data met several key assumptions required for its application. First, the study involved three or more independent variables, making the Friedman test an appropriate choice for comparing multiple conditions or groups. Second, the sampling process was random, ensuring that the data was not biased. Third, the dependent variable in this study was ordinal, which aligns with the requirement for

the Friedman test, as it is designed to handle non-parametric data of this type. Additionally, the data did not need to be normally distributed, further justifying the use of the Friedman test given the characteristics of the dataset. Therefore, this test was the most suitable statistical method for analyzing the differences across multiple conditions. Also, no outliers were checked, since outliers are data points that significantly deviate from most of the data. In the case of Likert scale data, the values are discrete and ordinal, and the scale has specific meaning and interpretation. Each value on the scale corresponds to a distinct response from the participants, and there is no continuous underlying measurement. The concept of outliers is more applicable to continuous variables where extreme values could be considered as potential outliers. In the case of Likert scale data, it is essential to preserve the integrity of the scale and respect the ordinal nature of the responses. For objective measures, the normality was checked using Q_Q plots, histograms and Shapiro-Wilk normality test. The data was not normalized therefore aligned rank transform for non-parametric factorial analysis using ANOVA was carried out. When these procedures are used on non-normal data, power is reduced and the probability of a type I error increases. The ART [31] procedure is a valuable method for non-parametric testing of both main effects and interactions using standard ANOVA techniques. Basic descriptive statistical analysis technique was also used to analyze objective measures in which mean, standard deviation, min and max for each angle of each task was computed and plotted as a bar graph. For testing the hypothesis 95 percent confidence level was considered. For graphical representation, bar plot was used to compare mean ratings.

The first step in the analysis was to determine the types of variables, categorizing them as either categorical, continuous, or ordinal. The questionnaire responses, measured using Likert scales, were treated as ordinal variables, reflecting their role in capturing subjective opinions and attitudes in a ranked format. All rating data from the Likert scales were converted into numeric form to facilitate statistical analysis. For each participant, an overall rating was calculated by averaging their responses across all relevant columns. This aggregation provided a comprehensive measure of each participant's experience and perceptions. Given the ordinal nature of the Likert scale data, non-parametric statistical tests were employed, which do not assume a normal distribution. Basic descriptive statistical analysis was conducted to provide a comprehensive overview of the data. Measures such as mean, standard deviation, minimum, and maximum values for each angle of each task were computed and visualized using bar graphs. These visualizations helped in comparing the mean ratings and identifying trends or patterns in the data. For graphical representation, bar plots were used to compare mean ratings across different conditions, providing clear and interpretable insights into the data.

5 Results

5.1 RQ1 – Task Performance

In the assembly line monitoring task, the analysis revealed a significant difference in total task time across the different camera angles, $F(2, 142) = 5.021$, $p = .007$. This result indicates that the time required to complete the task varied significantly depending on the camera angle used. Specifically, the data suggests that different angles impact task performance, highlighting the importance of camera angle selection in optimizing efficiency during monitoring tasks. This supports our hypothesis that different camera angles will affect task performance.

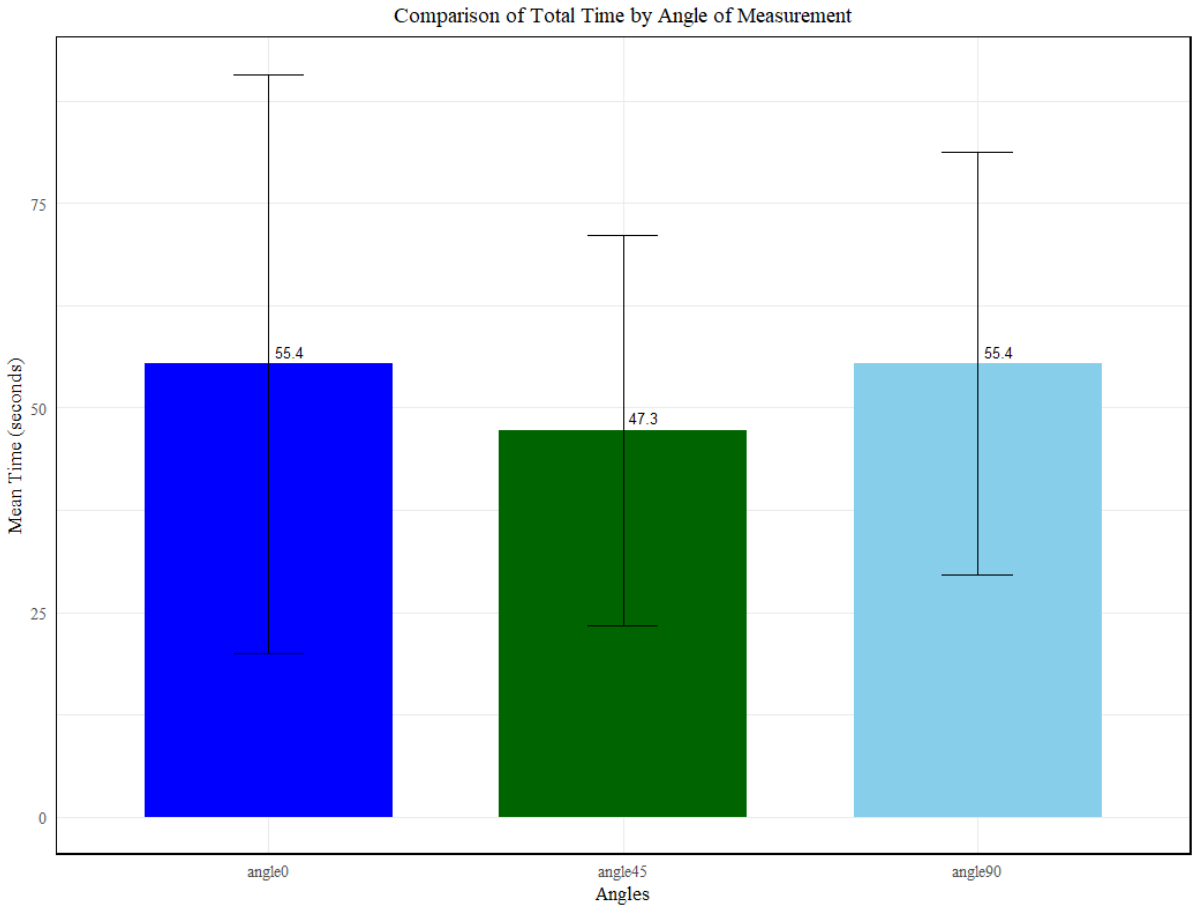

Figure 10. Total Time for Assembly Line Monitoring Task

The graphical representation in **Error! Reference source not found.** illustrates the mean and standard deviation for each of the three angles, providing a visual comparison of the task completion times. From the graph, it is apparent that the mean task time for 45° angle is lower compared to 0° angle and 90° angle, suggesting that participants performed the task more efficiently with this camera angle.

contrast	***p* value**
0° angle - 45° angle	0.353
0° angle - 90° angle	0.339
45° angle - 90° angle	0.006

Table 1. Pairwise Comparison of Total Time

The post-hoc test used in this analysis is a pairwise comparison with Bonferroni adjustment for multiple comparisons. This test adjusts the *p*-values to ensure that the risk of falsely identifying a significant effect (Type I error) is minimized when multiple pairwise tests are conducted. The pairwise comparison results are summarized in Table 1. The comparison between the 45° angle and the 90° angle revealed a significant difference, with an estimated difference of -17.93 seconds (*SE* = 5.66), a *t*-ratio of -3.169, and a *p*-value of .006. For the comparisons between 0° angle and 45° angle the estimated difference was 8.91 seconds (*SE* = 5.66), with a *t*-ratio of 1.575 and a *p*-value of .353, suggesting no significant difference. For the comparison between 0° angle and 90° angle, the difference was -9.02 seconds (*SE* = 5.66), with a *t*-ratio of -1.594 and a *p*-value of .339, also indicating no significant difference. This suggests that while 0° angle and 45° angle, and 0° angle and 90° angle, did not significantly differ in task performance time, 45° angle and 90° angle did.

Considering the errors detected in the assembly line monitoring task, the analysis revealed a significant difference of angles on errors, $F(2,142)=78.731$, $p < 0.001$. This indicates that different camera angles can affect the number of errors detected. This supports our hypothesis that different camera angles will affect task performance.

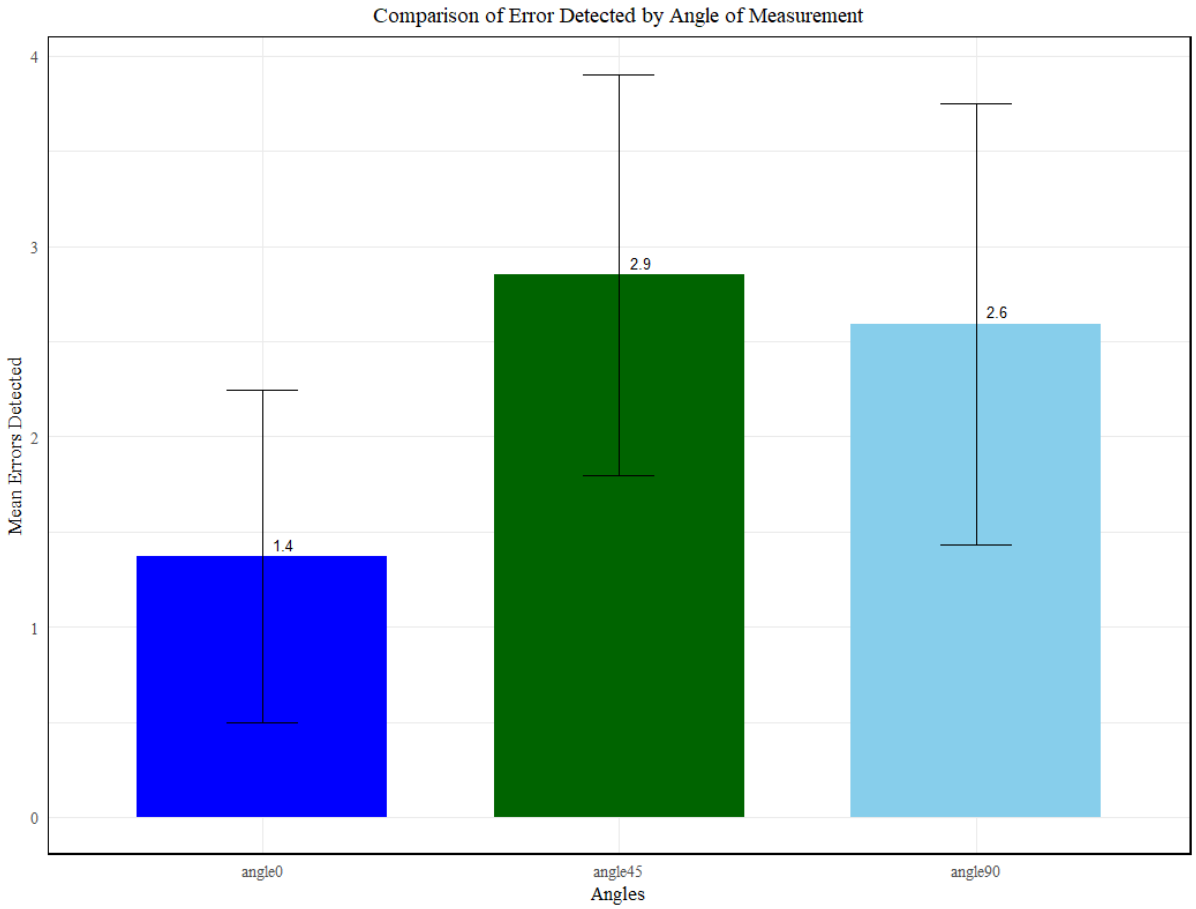

Figure 11. Comparison of Error Detected by Angle

The graphical representation in Figure 11 illustrates the mean and standard deviation for errors detected at each of the three angles, providing a visual comparison. From the graph, it is apparent that the mean of error detected for 45° angle is higher compared to 0° angle and 90° angle, suggesting that participants performed the task more efficiently with this camera angle.

contrast	***p* value**
0° angle - 45° angle	<0.001
0° angle - 90° angle	<0.001
45° angle - 90° angle	0.003

Table 2. Pairwise Comparison of Error Detected

Furthermore, a post-hoc test used in this analysis is a pairwise comparison with Bonferroni adjustment for multiple comparisons. This test adjusts the *p*-values to ensure that the risk of falsely identifying a significant effect (Type I error) is minimized when multiple pairwise tests are conducted. The pairwise comparison results are summarized in Table 2. The comparisons between 0° angle and 45° angle yielded an estimated difference of -57.3 errors (*SE* = 4.8), with a *t*-ratio of -11.941 and a *p*-value < .001. Comparing angle 0° and angle 90°, the estimated difference was -44.7 errors (*SE* = 4.8), with a *t*-ratio of -9.311 and *p*-value < .001. This result demonstrates that the error rate at angle0 was significantly lower than at angle90. The comparison between angle 45° and angle 90° showed an estimated difference of 12.6 errors (*SE* = 4.8), with a *t*-ratio of 2.630 and a *p*-value of .003, revealing a significant difference in error rates, with angle45 resulting in a higher error rate compared to angle90.

Metrics	***p*-value**	**0° angle**		**45° angle**		**90° angle**	
		M	***SD***	**M**	***SD***	**M**	***SD***
Total Time	0.007	55.4	35.38	47.3	23.81	55.4	25.78
Errors Detected	<0.001	1.4	0.87	2.9	1.05	2.6	1.15

Table 3. Task Performance Metrics for Assembly Line Monitoring Task

Table 3 presents a comprehensive analysis of the assembly line monitoring task across three different camera angles: 0°, 45°, and 90°. The metrics analyzed include total time and errors detected, with corresponding *p*-values, mean values (*M*), and standard deviations (*SD*) for each angle.

5.1.1 Total Time

- The *p*-value for total time is 0.007, indicating statistically significant differences in task completion times across the three angles. This supports the hypothesis that different camera angles affect task performance.
- Mean values show that the 45° angle had the shortest average completion time of 47.3 seconds, suggesting better efficiency. Both the 0° and 90° angles had a mean completion time of 55.4 seconds.

5.1.2 Errors Detected

- The *p*-value for errors detected is extremely low ($p < 0.001$), demonstrating a highly significant difference in error detection across the angles.
- Mean values for errors detected indicate that the 45° angle had the highest average number of errors detected ($M = 2.9$), followed by the 90° angle ($M = 2.6$), and the 0° angle with the fewest errors detected ($M = 1.4$).

The 45° angle demonstrates a balance between efficiency and error detection, having the lowest mean total time and the highest mean errors detected. This suggests that the 45° angle may provide an optimal viewpoint for monitoring tasks. Total task time ($p < 0.001$) for assembly line monitoring task shows significant differences among the three camera angles. The result indicates that the hypothesis that different camera angles affect task performance is supported, with statistically significant differences in task completion times across the three angles.

Considering the total time for drone delivery task, the analysis revealed a significant difference of angles on total task time $F(2,142) = 13.634$, $p < .001$. This indicates that different camera angles affect the total task time in drone delivery task as well.

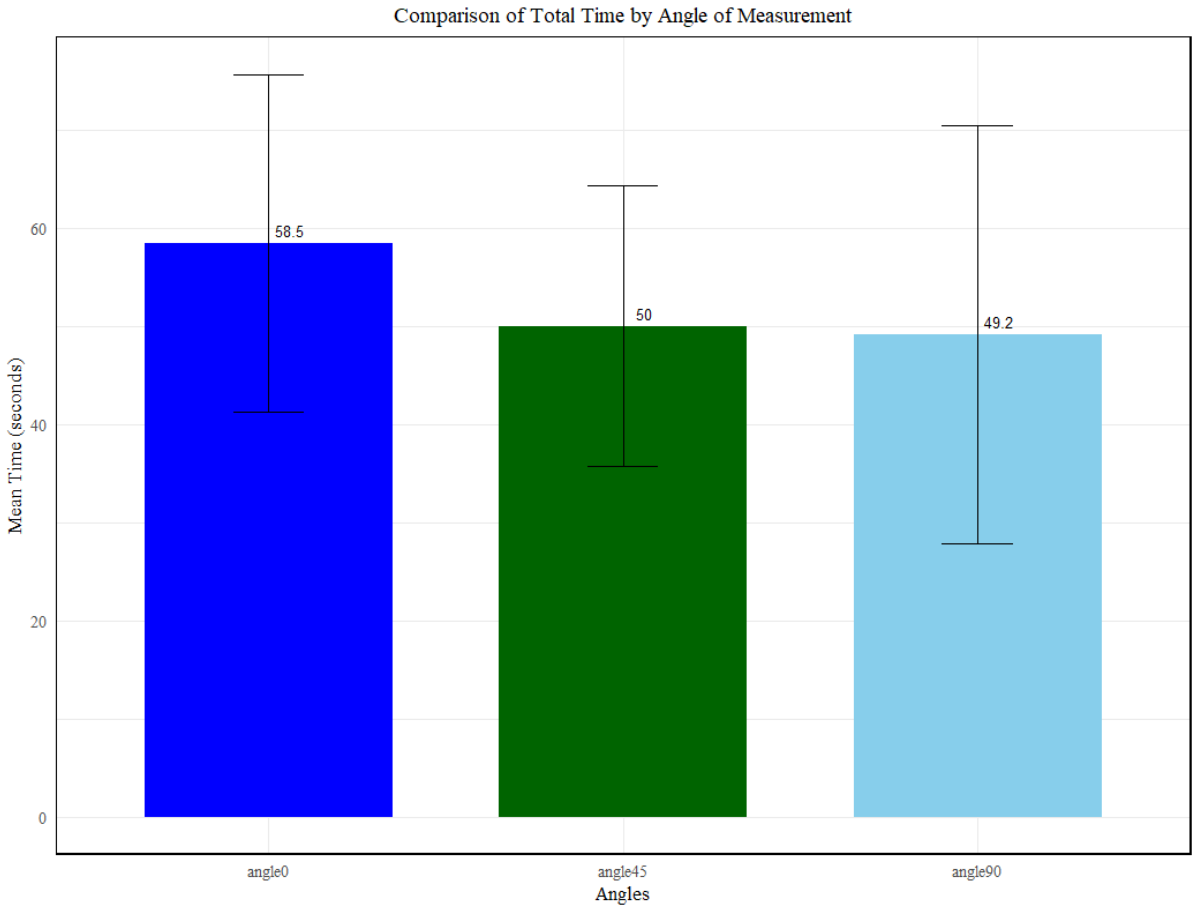

Figure 12. Comparison of Total Time in Delivery Task

The graphical representation in Figure 12 illustrates the mean and standard deviation for errors detected at each of the three angles. The mean values suggest that the 90° angle had the shortest average completion time, followed closely by the 45° angle, while the 0° angle had the longest average completion time.

contrast	***p* value**
0° angle - 45° angle	0.0006
0° angle - 90° angle	<0.001
45° angle - 90° angle	0.7128

Table 4. Pairwise Comparison of Total Time in Drone Delivery Task

The post-hoc test for pairwise comparison with Bonferroni adjustment provides further insight into the significance of these differences. The comparison between 0° angle and 45° yielded an estimated difference of 30.5 seconds (*SE* = 8.01), with a *t*-ratio of 3.811 and a *p*-value of *p* =.0006, showing that task completion time was significantly shorter at 0° angle compared to 45° angle. The comparison between 0° angle and 90° showed the estimated difference was 40.0 seconds (*SE* = 8.01), with a *t*-ratio of 4.997 and a *p*-value of *p* < .0001. This result indicates that task completion time at 0° angle was significantly shorter than at 90° angle. The comparison between 45° angle and 90° angle showed an estimated difference of 9.5 seconds (*SE* = 8.01), with a *t*-ratio of 1.186 and a *p*-value of *p* =.7128. This difference was not statistically significant, indicating no meaningful difference in task completion time between 45° angle and 90° angle.

Considering the time taken to pick up the package in drone delivery task, the analysis revealed a significant main effect of angles on pickup time, *F*(2,142) = 7.539, *p* =.0008, indicating that pickup times differed significantly across the different camera angles. This indicates that the hypothesis that different camera angles affect the time taken to pick up the package is supported by the data.

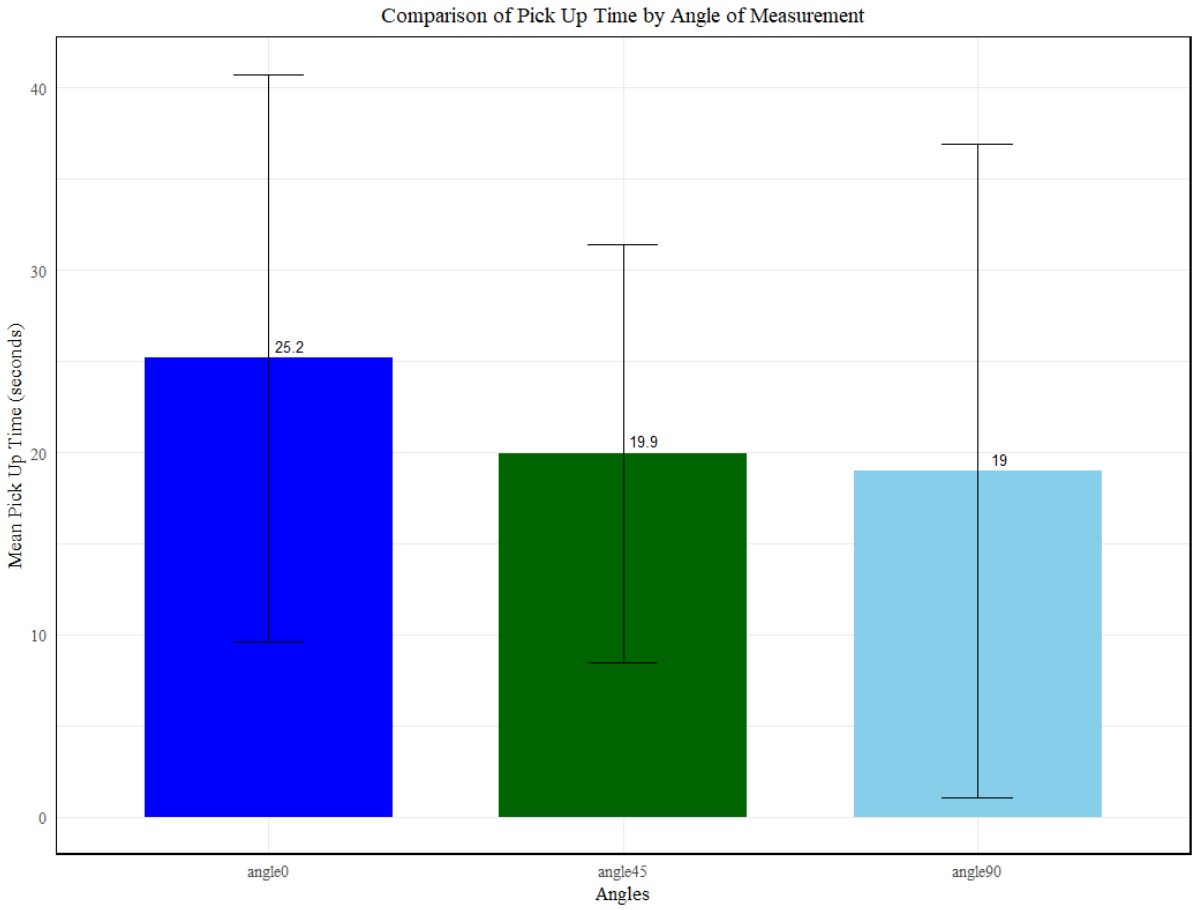

Figure 13. Comparison of Pick Up Time by Angle

The graphical representation in Figure 13 illustrates the mean and standard deviation for errors detected at each of the three angles. The mean values suggest that the 90° angle allowed participants to pick up the package in the shortest amount of time, followed closely by the 45° angle, while the 0° angle resulted in the longest average time.

contrast	***p* value**
0° angle - 45° angle	0.0575
0° angle - 90° angle	0.0005
45° angle - 90° angle	0.4236

Table 5. Pairwise Comparison of Pick-Up Time

The post-hoc test for pairwise comparisons with Bonferroni adjustment provides further detail on these differences. The comparison between 0° angle and 45° angle showed an estimated difference of 20.0 seconds (*SE* = 8.46), with a *t*-ratio of 2.369 and a *p*-value of *p* =.0575. Although this difference approached significance, it did not meet the threshold for statistical significance after adjustment. This implies that while there is a noticeable difference in the time taken between these two angles. For the comparison between 0° angle and 90° angle, estimated difference was 32.6 seconds (*SE* = 8.46), with a *t*-ratio of 3.849 and a *p*-value of *p* =.0005. This result indicates that pickup time was significantly shorter at 0° angle compared to 90° angle. The comparison between 45° angle and 90° angle resulted in an estimated difference of 12.5 seconds (*SE* = 8.46), with a *t*-ratio of 1.480 and a *p*-value of *p* =.4236. This difference was not statistically significant, suggesting no meaningful difference in pickup. The analysis reveals that the 90° angle is the most effective in reducing the time taken to pick up the package, with a statistically significant difference compared to the 0° angle. The 45° angle also shows an improvement over the 0° angle, but this difference is not statistically significant. There is no significant difference in pick-up time between the 45° and 90° angles, indicating that both can be effective choices for optimizing task performance in this aspect.

For the time taken to drop off the package in drone delivery task, results revealed a significant main effect of angles on drop-off time, $F(2,142) = 5.629$, $p = .0044$, indicating that drop-off times varied significantly across the different camera angles.. This indicates that the hypothesis that different camera angles affect the time taken to drop off the package is significant.

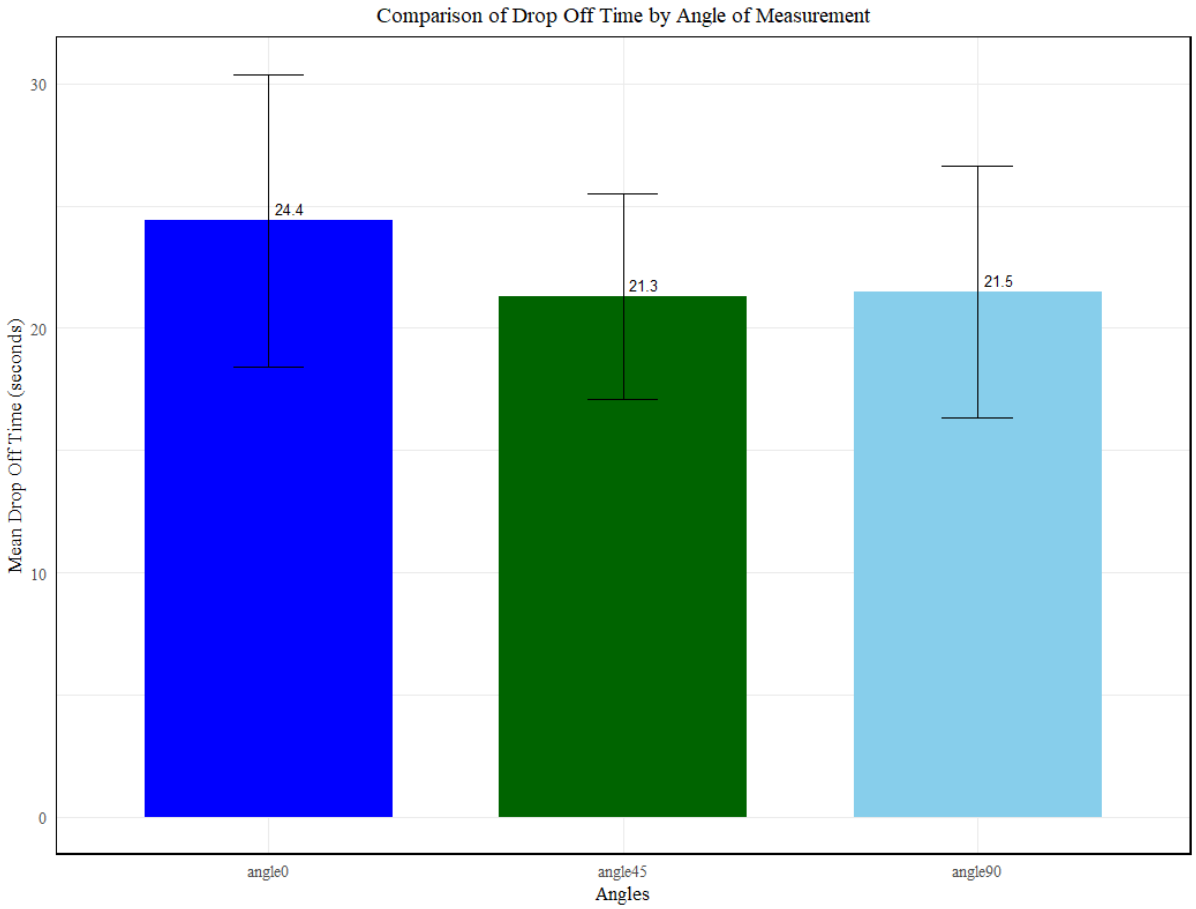

Figure 14. Comparison of Drop Off Time by Angle

The graphical representation in Figure 14 illustrates the mean and standard deviation for errors detected at each of the three angles. From the mean values, it is evident that the 45° and 90° angles are associated with shorter drop-off times compared to the 0° angle. Specifically, the 45° and 90° angles both result in similar and reduced times for dropping off the package, as compared to the 0° angle.

contrast	***p* value**
0° angle - 45° angle	0.0124
0° angle - 90° angle	0.0131
45° angle - 90° angle	1.0000

Table 6. Pairwise Comparison of Drop Off Time

Post-hoc test for pairwise comparisons with Bonferroni adjustment provide additional insights into these differences. The comparison between 0° angle and 45° angle revealed an estimated difference of 25.130 seconds (*SE* = 8.62), with a *t*-ratio of 2.914 and a *p*-value of *p* =.0124. This indicates that drop-off time was significantly shorter at 0° angle compared to 90° angle. The comparison between 0° angle and 90° angle yielded an estimated difference of 24.981 seconds (*SE* = 8.62), with a *t*-ratio of 2.897 and a *p*-value of *p*=.0131. This also demonstrates a significantly shorter drop-off time at 0° angle compared to 90° angle. The comparison between 45° angle and 90° angle resulted in an estimated difference of -0.148 seconds (*SE* = 8.62), with a *t*-ratio of -0.017 and a *p*-value of *p* =1.000. This result indicates no significant difference in drop-off time between 45° angle and 90° angle. The analysis reveals that both the 45° and 90° camera angles are more effective than the 0° angle in reducing the time taken to drop off the package, with significant differences observed between the 0° angle and each of the other two angles. However, there is no significant difference in drop-off time between the 45° and 90° angles, indicating that either of these angles could be used effectively to optimize performance in this task.

For the distance to target drop-off location in drone delivery task, results revealed a significant main effect of camera angles on distance, $F(2,142) = 21.142$, $p < .001$, indicating that the distance varied significantly across the different camera angles. This indicates that the hypothesis that different camera angles affect the distance from the target drop-off location is strongly supported by the data.

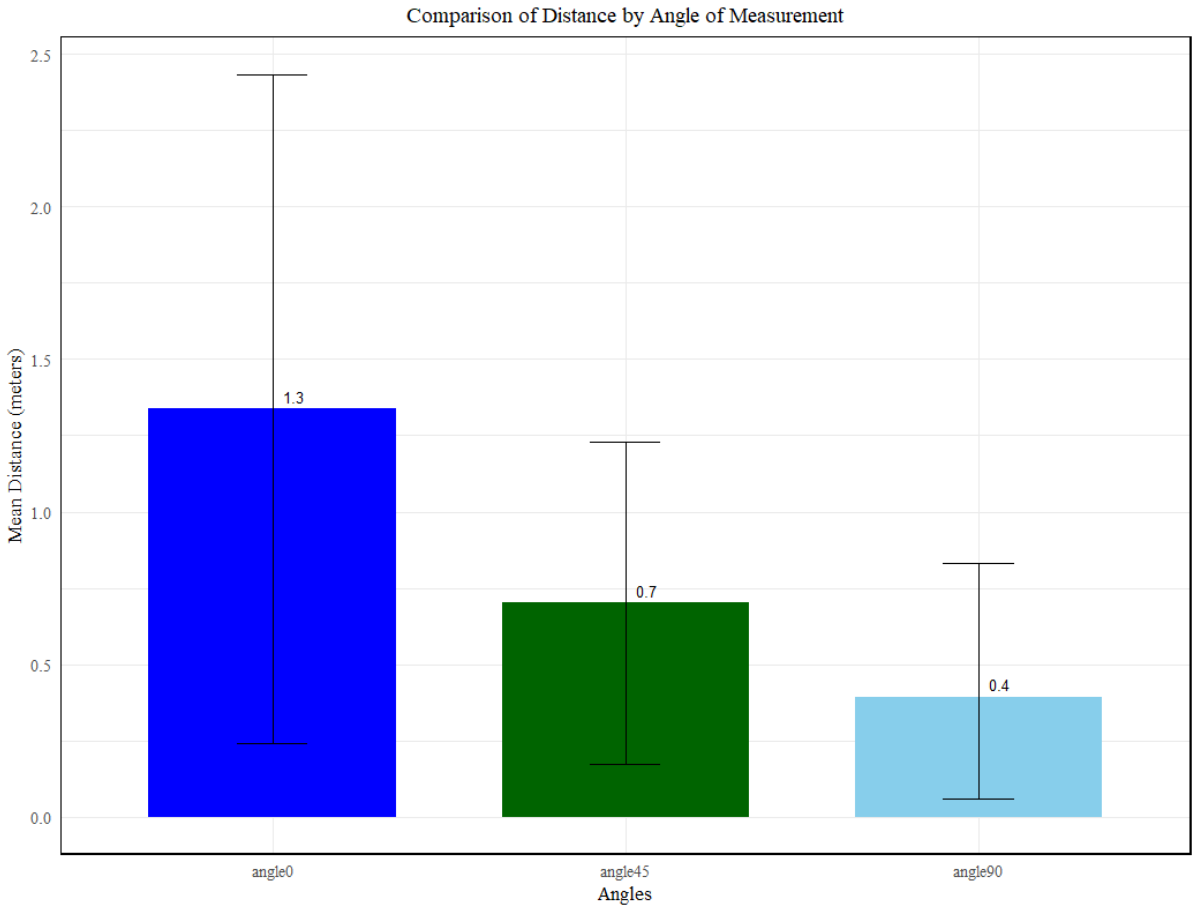

Figure 15. Comparison of Distance by Angle

The graphical representation in Figure 15 illustrates the mean and standard deviation for errors detected at each of the three angles. The mean values show that the distance to the target decreases as the camera angle changes from 0° to 90°. Specifically, the 90° angle results in the smallest mean distance from the target, suggesting the highest accuracy in reaching the drop-off location, followed by the 45° angle, and then the 0° angle, which has the largest mean distance.

contrast	***p* value**
0° angle - 45° angle	0.0190
0° angle - 90° angle	<0.001
45° angle - 90° angle	0.0009

Table 7. Pairwise Comparison of Distance to Target

The post-hoc test for pairwise comparison with Bonferroni adjustment provides further insight into the significance of these differences. The comparison between 0° angle and 45° angle revealed an estimated difference of 21.8 units (*SE* = 7.85), with a *t*-ratio of 2.771, *p* =.019. This indicates that the distance at 0° angle was significantly different from 45° angle. The comparison between 0° angle and 90° angle yielded an estimated difference of 50.9 units (*SE* = 7.85), with a *t*-ratio of 6.480, *p* < .001. This demonstrates a significantly larger distance at 0° angle compared to 90° angle. The comparison between 45° angle and 90° angle showed an estimated difference of 29.1 units (*SE* = 7.85), with a *t*-ratio of 3.709, *p* =.0009. This indicates a significant difference in distance between 45° angle and 90° angle. The analysis demonstrates that camera angles significantly impact the accuracy of reaching the target drop-off location in drone delivery tasks. The 90° angle consistently results in the smallest distance from the target, indicating the highest level of precision. Both the 45° and 90° angles outperform the 0° angle in reducing the distance from the target, with the 90° angle showing the best performance in terms of accuracy.

Metrics	*p* value	0° angle		45° angle		90° angle	
		M	***SD***	**M**	***SD***	**M**	***SD***
Total Time	<0.001	58.5	17.17	50	13.64	49.2	21.27
Pick up Time	0.0007	25.2	15.55	19.9	10.85	19	17.90
Drop Off Time	0.0044	24.4	5.99	21.3	4.08	21.5	5.16
Distance to Target	<0.001	1.3	1.09	0.7	0.52	0.4	0.43

Table 8. Task Performance Metrics for Drone Delivery Task

The results in Table 8 summarizes the performance metrics for the drone delivery task, including total time, pick-up time, drop-off time, and distance to the target across three camera angles: 0, 45, and 90°. The *p*-values indicate the statistical significance of differences in these metrics between angles. Total time ($p < 0.001$) indicates that the time required to complete the task differs across camera angles. The mean total time is longest at the 0° angle (M =58.5 seconds) and shortest at the 90° angle (M =49.2 seconds), with the 45° angle falling in between (M =50 seconds). This suggests that the 90° angle is the most efficient for completing the task. Pick-up time ($p = 0.0007$) confirms a significant difference among the angles. The mean pick-up time is shortest at the 90° angle (M =19 seconds), indicating improved efficiency compared to the 0° angle (M =25.2 seconds) and the 45° angle (M =19.9 seconds). In terms of drop-off time, the *p*-value of ($p = 0.0044$) shows a significant difference, with the 45° angle demonstrating the shortest mean drop-off time (M =21.3 seconds), followed closely by the 90° angle (M =21.5 seconds). The 0° angle has the longest mean drop-off time (M =24.4 seconds), and the 45° angle also exhibits the smallest standard deviation (SD = 4.08 seconds), indicating consistent performance. Finally, the distance to the target has a *p*-value of 9.18e-09, indicating a highly significant difference. The 90° angle achieves the shortest mean distance to the target (M =0.4 meters), suggesting the highest accuracy, while the 0° angle results in the longest mean distance (M =1.3 meters) whereas 45° angle falls in between (M =0.7 meters).

5.2 RQ2 - Situation Awareness

For the Assembly Line Monitoring task, situation awareness data was collected using the Situation Awareness Rating Technique (SART) questionnaire to assess various metrics such as instability,

complexity, variability, arousal, concentration, division, mental capacity, information quantity, and familiarity. The analysis revealed that only instability and complexity showed significant differences between camera angles, with *p*-values of 0.0130 and 0.0041, respectively. This indicates that the camera angles had a notable impact on these aspects of situation awareness.

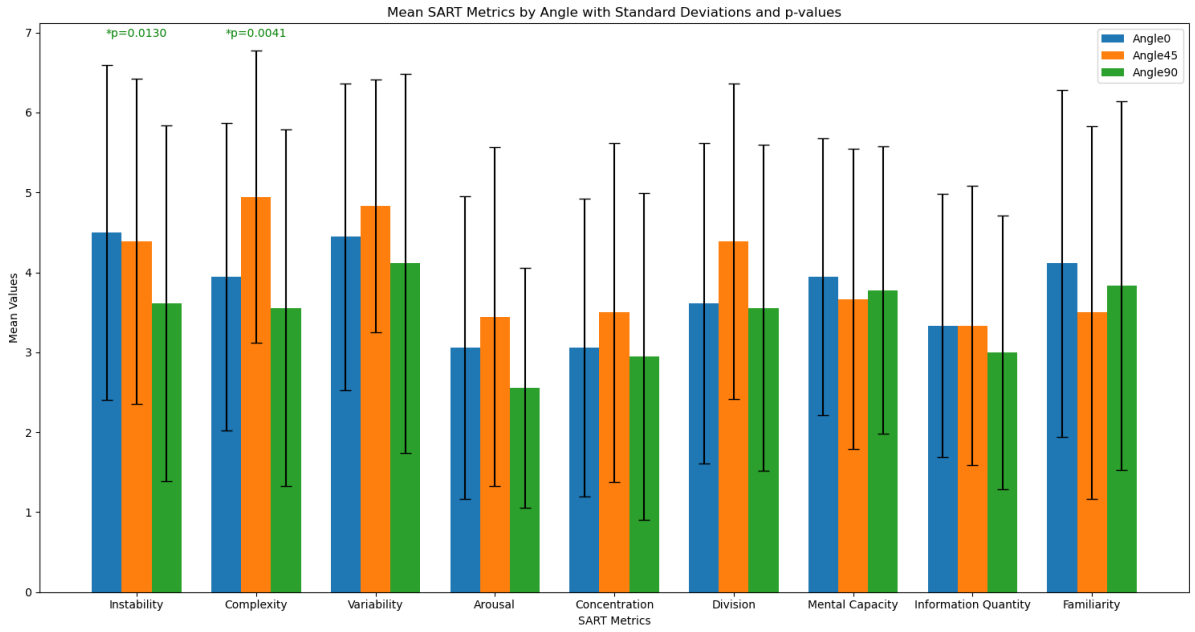

Figure 16. SART Metrics by Angle in Assembly Line Monitoring Task

The graphical representation in Figure 16 illustrates the mean and standard deviation for SART metrics at each of the three angles. The graphical representation shows that only instability and complexity metrics have significant differences.

Metrics	***p*-value**	**0° angle**		**45° angle**		**90° angle**	
		M	***SD***	**M**	***SD***	**M**	***SD***
Instability	0.013	4.50	2.09	4.38	2.03	3.61	2.22
Complexity	0.004	3.94	1.92	4.94	1.83	3.55	2.22
Variability	0.147	4.44	1.91	4.83	1.58	4.11	2.37
Arousal	0.312	3.05	1.89	3.44	2.12	2.55	1.50
Concentration	0.569	3.05	1.86	3.50	2.12	2.94	2.04
Division	0.087	3.61	2.00	4.38	1.97	3.55	2.03
Mental Capacity	1.000	3.94	1.73	3.66	1.87	3.77	1.80
Information Quantity	0.667	3.33	1.64	3.33	1.74	3.00	1.71
Familiarity	0.663	4.11	2.16	3.50	2.33	3.83	2.30

Table 9. SART Metrics for Assembly Line Monitoring Task

The results in Table 9 shows the Mean (M) and Standard Deviations (*SD*) for each SART metric across the three camera angles: 0, 45, and 90°, along with their respective p-values. The analysis of instability and complexity metrics reveals significant effects of camera angles in the Assembly Line Monitoring task. For instability, a *p*-value of $p = 0.0130$, indicates a significant impact of camera angle. The mean instability scores are higher at 0° angle ($M = 4.50$) and 45° angle ($M = 4.38$) compared to 90° angle ($M = 3.61$), with relatively high standard deviations suggesting variability in responses. For complexity, the *p*-value of 0.0041 signifies a significant difference between angles, with the highest mean complexity at 45° angle ($M = 4.94$), followed by 0° angle ($M = 3.94$) and 90° angle ($M = 3.55$). The standard deviations for complexity also show considerable variation, especially at 45° angle. In contrast, metrics such as variability, arousal, concentration, division, mental capacity, information quantity, and familiarity indicate no significant differences across the angles. The mean values and standard

deviations for these metrics remain relatively stable, reflecting consistent responses regardless of the camera angle.

Contrast	**Instability *p* values**	**Complexity *p* values**
0° angle - 45° angle	0.8574	0.0932
0° angle - 90° angle	0.0332	0.6668
45° angle - 90° angle	0.1122	0.0099

Table 10. Pairwise Comparison for Instability and Complexity

The post-hoc Nemenyi test for pairwise comparison provides further insights into the significant metrics. For instability, the p-value between 0° angle and 45° angle is 0.8574, indicating no significant difference. However, a significant difference is observed between 0° angle and 90° angle, with a *p*-value of 0.0332, suggesting higher instability at 0° angle. The comparison between 45° angle and 90° angle shows no significant difference ($p = 0.1122$). For complexity, the comparison between 0° angle and 45° angle shows a trend towards significance ($p = 0.0932$), with higher complexity at 45° angle. No significant difference is found between 0° angle and 90° angle ($p = 0.6668$). However, there is a significant difference between 45° angle and 90° angle, with a *p*-value of $p = 0.0099$, indicating notably higher complexity at 45° angle compared to 90° angle. Overall, these results indicate that while instability and complexity are significantly affected by the camera angle, other metrics such as variability, arousal, and concentration do not show significant differences. The pairwise comparisons further clarify where these significant differences lie, particularly highlighting the higher complexity and instability associated with specific angles.

Considering the Drone Delivery task, the *p*-values for complexity and variability are $p = 0.0109$ and $p = 0.0090$, respectively, indicating significant differences in these metrics based on camera angles.

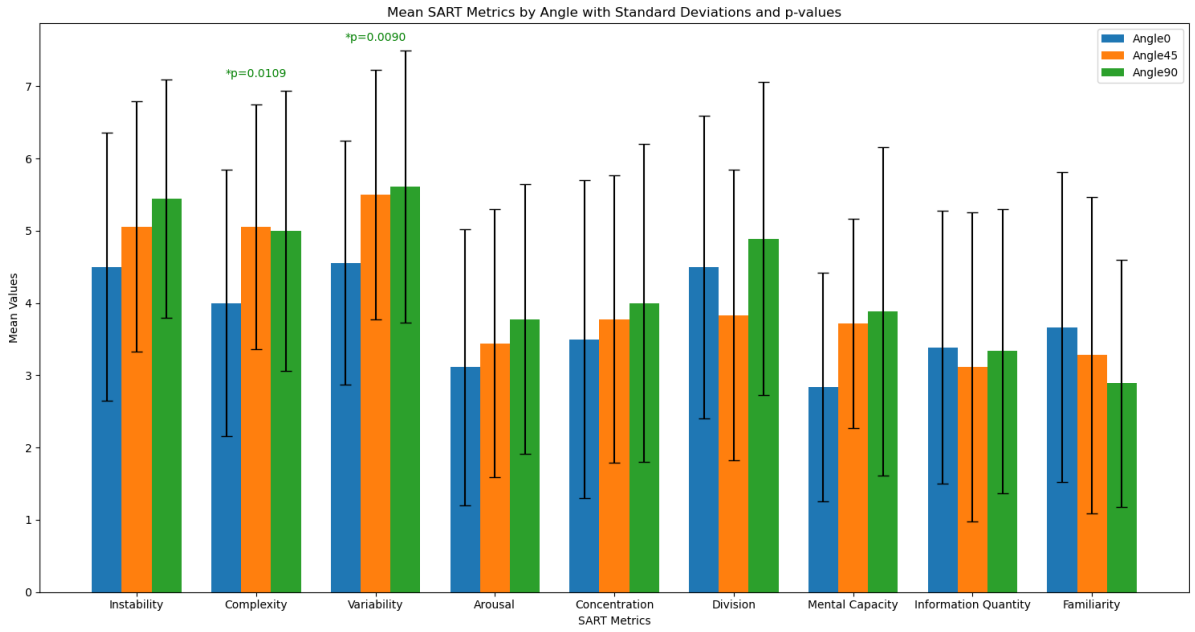

Figure 17. SART Metrics by Angle in Drone Delivery Task

The graphical representation in Figure 17 shows the mean and standard deviation for each metric across the three angles, highlighting where significant differences exist. It shows that only complexity and variability metrics have significant differences.

Metrics	***p*-value**	**0° angle**		**45° angle**		**90° angle**	
		M	***SD***	**M**	***SD***	**M**	***SD***
Instability	0.1353	4.50	1.85	5.05	1.73	5.44	1.65
Complexity	0.0109	4.00	1.84	5.05	1.69	5.00	1.94
Variability	0.0090	4.55	1.68	5.50	1.72	5.61	1.88
Arousal	0.1769	3.11	1.90	3.44	1.85	3.77	1.86
Concentration	0.4042	3.50	2.20	3.77	1.98	4.00	2.19
Division	0.0691	4.50	2.09	3.38	2.00	4.88	2.16
Mental Capacity	0.4667	2.83	1.58	3.72	1.44	3.88	2.27
Information Quantity	0.6832	3.38	1.88	3.11	2.13	3.33	1.97
Familiarity	0.5292	3.66	2.14	3.27	2.19	2.88	1.71

Table 11. SART Metrics for Drone Delivery Task

The results in Table 11 summarizes the analysis of various metrics for the Drone Delivery task. For instability (p = 0.135), there is no significant difference across angles, though mean instability scores increase slightly from 0° angle (M =4.50) to 45° angle (M =5.05) and 90° angle (M =5.44), with standard deviations indicating variability. Complexity shows a significant difference (p =0.010), with the mean highest at 45° angle (M =5.05), followed by 90° angle (M =5.00) and 0° angle (M =4.00), indicating increased perceived complexity at specific angles. Variability also shows a significant difference (p =0.009), with the highest mean at 90° angle (M =5.61), followed by 45° angle (M =5.50) and 0° angle (M =4.55). Other metrics such as arousal (p =0.176), concentration (p =0.404), division (p =0.069), mental capacity (p =0.4667), information quantity (p =0.683), and familiarity (p =0.529) do not show significant differences across angles. Mean values for these metrics exhibit slight variations, with standard deviations suggesting consistent responses.

Contrast	Complexity *p*-value	Variability *p*-value
0° angle - 45° angle	0.7706	0.2531
0° angle - 90° angle	0.0513	0.0209
45° angle - 90° angle	0.9000	0.5237

Table 12. Pairwise Comparison for Complexity and Variability

The post-hoc Nemenyi test for pairwise comparison provides further insights into the significant metrics. For complexity, the *p*-value between 0° angle and 45° angle is $p = 0.770$, indicating no significant difference, while the *p*-value between 0° angle and 90° angle is $p = 0.0513$, nearing significance, and the *p*-value between 45° angle and 90° angle is $p = 0.900$, indicating no significant difference. For variability, the *p*-value between 0° angle and 45° angle is $p = 0.253$, showing no significant difference, while the *p*-value between 0° angle and 90° angle is $p = 0.020$, indicating a significant difference, and the *p*-value between 45° angle and 90° angle is $p = 0.523$, indicating no significant difference. The analysis highlights that while complexity and variability are significantly influenced by the camera angle, other metrics such as arousal, concentration, division, mental capacity, information quantity, and familiarity do not show significant differences. The pairwise comparisons clarify these findings, particularly emphasizing the significant impact of camera angles on perceived complexity and variability in the Drone Delivery task.

5.3 RQ3 - Workload

Considering the assembly line monitoring task, workload data was collected using the NASA RTLX questionnaire, which measures various workload dimensions such as mental demand, physical demand, temporal demand, performance, effort, and frustration. The analysis revealed significant differences for mental demand ($p = 0.009$), physical demand ($p = 0.0002$), performance ($p = 0.112$), and effort ($p = 0.0104$), indicating that the camera angle significantly affects these metrics.

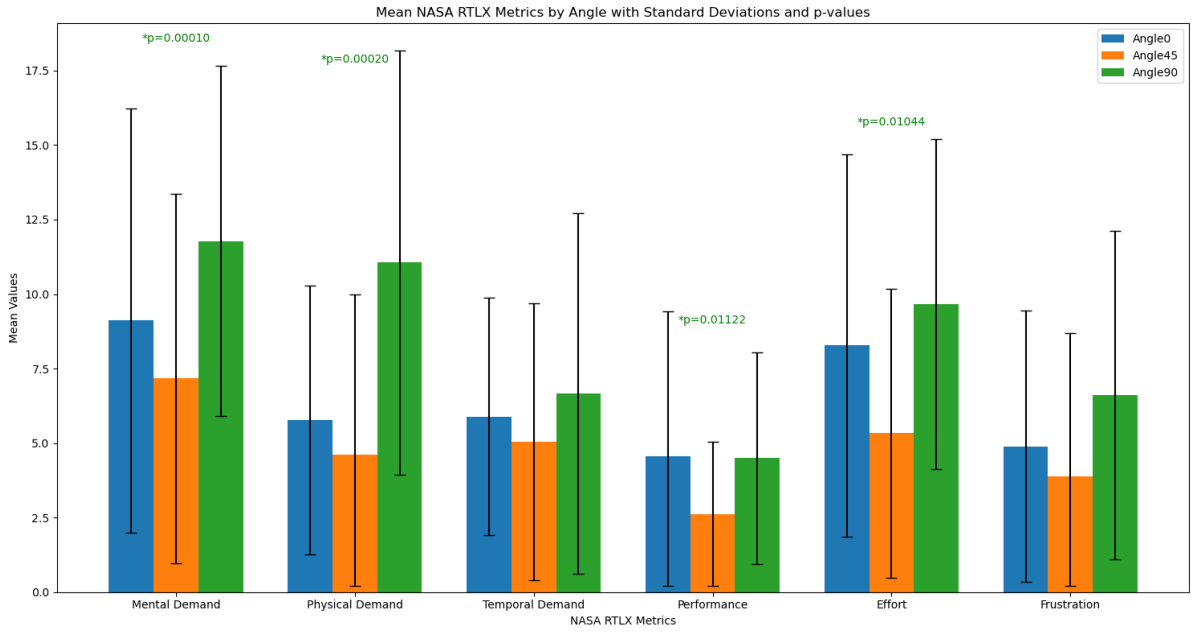

Figure 18. NASA RTLX Metrics by Angle in Assembly Line Monitoring Task

The graphical representation in Figure 18 shows the mean and standard deviation for each metric across the three angles, highlighting where significant differences exist.

Metrics	***p*-value**	**0° angle**		**45° angle**		**90° angle**	
		M	***SD***	**M**	***SD***	**M**	***SD***
Mental Demand	0.0009	9.11	7.11	7.16	6.19	11.77	5.87
Physical Demand	0.0002	5.77	4.50	4.61	5.38	11.05	7.11
Temporal Demand	0.6170	5.88	3.98	5.05	4.64	6.66	6.05
Performance	0.0112	4.55	4.86	2.61	2.42	4.50	3.55
Effort	0.0104	8.27	6.41	5.33	4.85	9.66	5.54
Frustration	0.0797	4.88	4.54	3.88	4.81	6.61	5.50

Table 13. NASA RTLX Metrics for Assembly Line Monitoring Task

The results in Table 13 summarizes the results for each metric across the three angles. Mental demand shows a significant difference, with a p-value of (p =0.0009), and the mean scores are (M =9.11) for 0° angle, (M =7.16) for 45° angle, and (M =11.77) for 90° angle. Physical demand also shows a significant difference with a p-value of (p = 0.0002), and the means are (M =5.77) for 0° angle, (M =4.61) for 45° angle, and (M =11.05) for 90° angle. Temporal demand (p =0.6170) does not show a significant difference, and the means are relatively close: (M =5.88) for 0° angle, (M =5.05) for 45° angle, and (M =6.66) for 90° angle. Performance has a significant difference with a p-value of (p = 0.0112), and the means are (M =4.55) for 0° angle, (M =2.61) for 45° angle, and (M =4.50) for 90° angle. Effort also shows a significant difference with a p-value of (p =0.0104), with means of (M =8.27) for 0° angle, (M =5.33) for 45° angle, and (M =9.66) for 90° angle. Frustration does not show a significant difference, with a p-value of (p = 0.0797) and means of (M =4.88) for 0° angle, (M =3.88) for 45° angle, and (M =6.61) for 90° angle.

Contrast	**Mental Demand *p*-value**	**Physical Demand *p*-value**	**Performance *p*-value**	**Effort *p*-value**
0° angle - 45° angle	0.3328	0.5237	0.1589	0.2183
0° angle - 90° angle	0.0209	0.0264	0.8098	0.4749
45° angle - 90° angle	0.0010	0.0010	0.0414	0.0128

Table 14. Pairwise Comparison for Mental Demand, Physical Demand, Performance and Effort

The post-hoc Nemenyi test for pairwise comparison provides further insights into the significant metrics. For mental demand, the p-values indicate no significant difference between 0° angle and 45° angle (p = 0.3328), but significant differences between 0° angle and 90° angle (p = 0.0209) and between 45° angle and 90° angle (p = 0.0010). For physical demand, the p-values show no significant difference between 0° angle and 45° angle (p = 0.5237), but significant differences between 0° angle and 90° angle (p = 0.0264) and between 45° angle and 90° angle (p = 0.0010). Performance shows no significant difference between 0° angle and 45° angle (p = 0.1589) and 0° angle and 90° angle (p = 0.8098), but a significant difference between 45° angle and 90° angle (p = 0.0414). Effort shows no significant difference between 0° angle and 45° angle (p = 0.2183) and 0° angle and 90° angle (p = 0.4749), but a significant difference between 45° angle and 90° angle (p = 0.0128).

Considering the drone delivery task, the p-values for mental demand ($p < 0.001$), physical demand ($p = 0.019$), performance ($p < 0.001$), effort, and frustration ($p < 0.001$) indicates that the given hypothesis is significant for these metrics only.

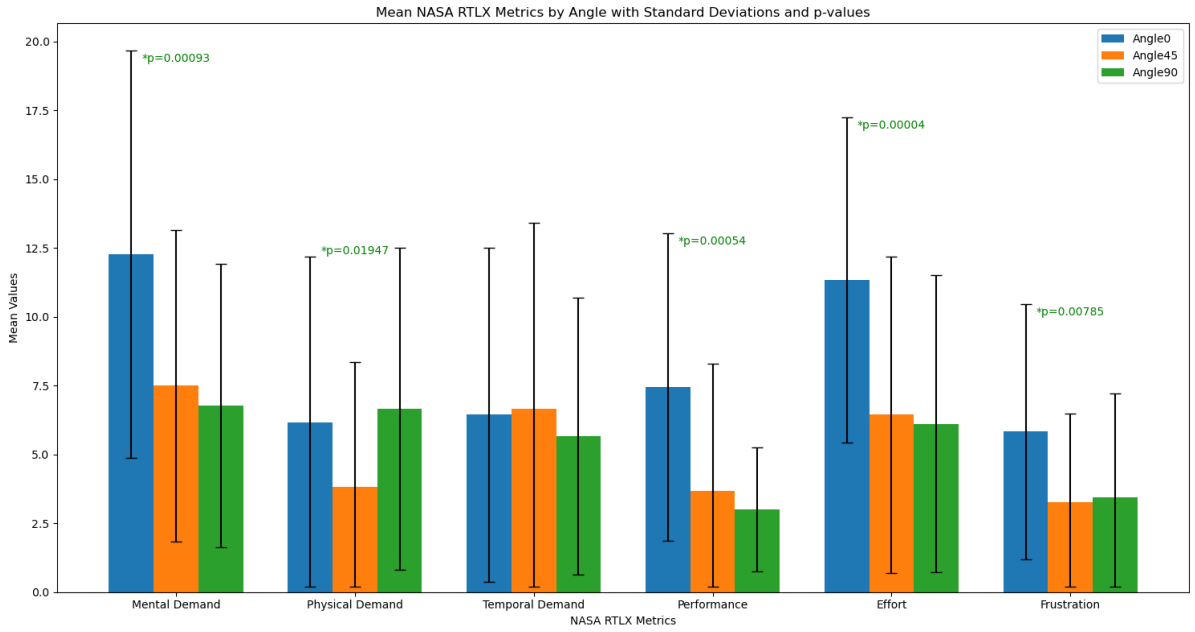

Figure 19. NASA RTLX Metrics by Angle in Drone Delivery Task

The graphical representation shows the mean and standard deviation for each metric across the three angles, highlighting where significant differences exist. Mental Demand, Physical Demand, Performance, Effort and Frustration have significant differences.

Metrics	***p*-value**	**0° angle**		**45° angle**		**90° angle**	
		M	***SD***	**M**	***SD***	**M**	***SD***
Mental Demand	0.00092	12.27	7.39	7.50	5.65	6.77	5.15
Physical Demand	0.01947	6.16	6.02	3.83	4.52	6.66	5.85
Temporal Demand	0.36787	6.44	6.07	6.66	6.73	5.66	5.04
Performance	0.00053	7.44	5.58	3.66	4.62	3.00	2.24
Effort	0.00004	11.33	5.90	6.44	5.75	6.11	5.38
Frustration	0.00784	5.83	4.63	3.27	3.21	3.44	3.77

Table 15. NASA RTLX Metrics for Drone Delivery Task

The results in Table 15 summarizes the results for each metric across the three angles. Mental demand ($p < 0.001$) shows a significant difference. It further reveals that mental demand for 0° angle (M =12.27, SD = 7.39), 45° angle (M =7.50, SD = 5.65), and 90° angle (M =6.77, SD = 5.15) affect the workload. Physical demand also shows a significant difference with a p-value of ($p = 0.019$), with mean scores of (M =6.16) for 0° angle, (M =3.83) for 45° angle, and (M =6.66) for 90° angle, and standard deviations of (SD = 6.02), (SD = 4.52), and (SD = 5.85). Temporal demand ($p = 0.3678$) does not show a significant difference, with mean scores of (M =6.44) for 0° angle, (M =6.66) for 45° angle, and (M =5.66) for 90° angle. Performance ($p < 0.001$) shows a significant difference with mean scores of (M =7.44) for 0° angle, (M =3.66) for 45° angle, and (M =3.00) for 90° angle. Effort ($p < 0.001$) shows a significant difference with mean scores of (M =11.33) for 0° angle, M =6.44 for 45° angle, and (M = 6.11) for 90° angle. Frustration ($p = 0.007$) also shows a significant difference with mean scores of (M = 5.83) for 0° angle, (M =3.27) for 45° angle, and (M =3.44) for 90° angle.

Contrast	**Mental Demand *p*-value**	**Physical Demand *p*-value**	**Performance *p*-value**	**Effort *p*-value**	**Frustration *p*-value**
0°angle - 45°angle	0.3325	0.0932	0.0076	0.0024	0.0513
0°angle - 90° angle	0.0013	0.9000	0.0164	0.0010	0.1339
45°angle-90°angle	0.5714	0.1339	0.9000	0.8098	0.9000

Table 16. Pairwise Comparison for Metrics with Significant Differences

The post-hoc Nemenyi test for pairwise comparison provides further insights into the significant metrics. For mental demand, the p-values indicate no significant difference between 0° angle and 45° angle (p = 0.3325), but significant differences between 0° angle and 90° angle (p = 0.0013), and no significant difference between 45° angle and 90° angle (p = 0.5714). For physical demand, the p-values show no significant difference between 0° angle and 45° angle (p = 0.0932) and 0° angle and 90° angle (p = 0.9000), and no significant difference between 45° angle and 90° angle (p = 0.1339). For performance, the p-values indicate significant differences between 0° angle and 45° angle (p = 0.0076) and between 0° angle and 90° angle (p = 0.0164), but no significant difference between 45° angle and 90° angle (p = 0.9000). For effort, the p-values indicate significant differences between 0° angle and 45° angle (p = 0.0024) and between 0° angle and 90° angle (p = 0.0010), but no significant difference between 45° angle and 90° angle (p = 0.8098). For frustration, the p-values indicate a trend towards significance between 0° angle and 45° angle (p = 0.0513), but no significant difference between 0° angle and 90° angle (p = 0.1339) or between 45° angle and 90° angle (p = 0.9000).

6 Discussion

The results from the Assembly Line Monitoring task demonstrate the substantial impact of different camera angles on various performance metrics. The analysis revealed that the total time spent monitoring the assembly line was significantly influenced by the camera angle, with a p-value of (p = 0.007) indicating significant difference. Specifically, 45° angle showed a notably lower mean time compared to angles 0° and 90°, highlighting its potential efficiency in this context. Additionally, the error detection metrics provided further insights, with 45° angle resulting in the highest errors detected, suggesting it might offer a clearer or more effective viewpoint for identifying issues which proves 45° angle as the best performer for assembly line monitoring. This significant difference ($p < 0.001$) shows the importance of optimal camera positioning to enhance task performance and accuracy in error detection. In the Drone Delivery task, the camera angle also proved to be a significant factor influencing performance metrics. The total time ($p < 0.001$) to complete the delivery was significantly different across the angles, indicating that angles 45° and 90° were more efficient compared to 0° angle. The post hoc test for pairwise comparisons further highlighted that 0° angle (M =58.5) took significantly more time than angles 45° (M =50) and angle 90° (M =49.2). This finding suggests that choosing the right angle can substantially reduce delivery time, enhancing operational efficiency. The analysis of the time taken to pick up and drop off packages reinforced these conclusions. For instance, the pick-up time (p = 0.0007) indicates significant differences among the angles, with angles 45° and 90° again showing more efficient performance. Similarly, the drop-off time analysis, with a p-value of (p = 0.0044), pointed out that angles 45° and 90° were significantly better compared to 0° angle.

The distance to the target drop-off location was another critical metric, with a highly significant ($p < 0.001$), suggesting that angles 45° and 90° allowed for more precise deliveries compared to 0° angle. These findings align well with previous research, such as Linnia Grip's work on vision-based object detection by drone [23]. In the experiments, the study tested three different camera angles for detecting a keyboard. The results indicated an F1 score of 0.93 for the camera looking straight down (equivalent to our 90° angle), 0.89 for the 45° angle, and 0.71 for the camera looking forward (equivalent to our 0° angle). This suggests that angles facing downward and at 45° provide better detection results than a forward-facing angle. Similarly, in our study, the angle 90° (M =2.9) and angle 45° (M =2.6) performed better in error detection on the assembly line compared to the 0° angle (M =1.4). In another experiment by Grip, she tested cup detection and found that most cups were detected at the 45° angle with an F1 score of 0.73, while the 0° angle had a lower F1 score of 0.4. This

parallels our findings where the 45° angle (*M* =2.9) outperformed other angles in error detection on the assembly line, further emphasizing the effectiveness of oblique angles for this task. Overall, the alignment between our study and Grip's research demonstrates that oblique camera angles 45° and downward-facing angles 90° significantly enhance error detection and efficiency in task performance. It also aligns with Masnadi et al. research on the effect of field of view on distance perception in virtual reality [29]. In the experiments, the study tested three different fields of view (FoV) for distance estimation tasks. The results indicated that users significantly underestimated distances with narrower FoVs, with a mean error of (*M* =-23.04) for the 60° FoV, (*M* =-8.32) for the 110° FoV, and (*M* =-0.56) for the 200° FoV. This suggests that different visual perspectives such as field of view and in our case camera angles affect distance perception. In drone delivery task study, the camera angles significantly influenced the accuracy of distance to the target. The results indicated that the 90° angle, which provides a more comprehensive view, resulted in the lowest mean distance error of (*M* =0.4), followed by the 45° angle (*M* =0.7) and the 0° angle (*M* =1.3). This parallels Masnadi et al.'s findings where wider FoVs resulted in lower distance estimation errors. Additionally, Masnadi et al. found significant differences in distance estimation errors across different FoVs, highlighting that narrower FoVs led to greater errors and less consistent performance. This finding is consistent with our study, where the 0° camera angle resulted in the highest mean distance error indicating less consistent performance compared to the 45° and 90° angles. Overall, the alignment between this research study and Masnadi et al.'s research demonstrates that wider fields of view or more optimal camera angles (such as 45° and 90°) significantly enhance distance estimation accuracy and consistency, reducing errors and improving task performance. This further emphasizes the importance of selecting appropriate visual perspectives to enhance the effectiveness of tasks involving distance estimation and navigation in both VR and real-world applications.

The Situation Awareness Rating Technique (SART) metrics further expanded on our findings, focusing on the user's situational awareness. The data indicated that instability (p = 0.0130) and complexity (p = 0.0041) were significantly affected by the camera angle. The post-hoc test for pairwise comparisons of these metrics revealed specific significant differences, particularly between angles 0° and 90° for instability, and angles 45° and 90° for complexity. These results highlight the critical role of camera angles in not only performance but also in maintaining situational awareness during monitoring tasks. The SART metrics for the Drone Delivery task also highlighted significant effects of camera angles on situational awareness. The metrics of complexity (p = 0.0109) and variability (p = 0.0090) indicate significant differences across the angles. 45° angle had the highest complexity, while 90° angle had the lowest variability. These results emphasize that different camera angles can distinctly impact how operators perceive and interact with their environment, affecting their situational awareness and

decision-making process during the drone delivery task. These findings align with previous research by Temma et al. on increasing situational awareness in third person piloting using a spatially coupled second drone [30]. The research demonstrated that situational awareness varies with different perspectives. They found that third-person piloting enhances situational awareness by providing an interactive third-person perspective from a spatially coupled second drone in the sky. Specifically, the bird's-eye view (similar to our 90° angle) significantly increased pilots' spatial comprehension around the primary drone, supporting existing knowledge on the effectiveness of this viewpoint. Additionally, their study highlighted that the manipulatable third-person perspective (TPP) was particularly useful for dynamic drone tasks around obstacles, paralleling our finding that the 45° angle (providing a balance between a downward and forward view) was most efficient for assembly line monitoring.

The NASA RTLX questionnaire results for the Assembly Line Monitoring task provided additional insights into the cognitive and physical demands associated with different camera angles. The p-values for mental demand, physical demand, performance, and effort indicate significant differences influenced by camera angle. The mean scores showed that 90° angle resulted in the highest mental and physical demands, while 45° angle was associated with the best performance and lower effort, suggesting it may be the most efficient and least demanding angle for operators. These findings highlight that camera angle selection can significantly affect user's workload and stress levels, which are crucial for maintaining high performance and user well-being. The NASA RTLX questionnaire results for the Drone Delivery task revealed significant impacts of camera angles on several workload metrics. The p-values for mental demand, physical demand, performance, effort, and frustration indicate significant differences. 0° angle had the highest mental and physical demands, while angles 45° and 90° were associated with better performance and lower effort and frustration. The mean scores and standard deviations reflected these variations, suggesting that camera angle selection is crucial for minimizing operator workload and enhancing overall task performance and satisfaction.

Overall, the results across different tasks and metrics consistently show that camera angle significantly affects performance, situational awareness, and workload. The post-hoc test for pairwise comparisons further elaborates on these findings, showing specific significant differences between angles that underscore the nuances of how camera perspectives can influence task outcomes. For instance, the significant difference in mental demand between angles 0° and 90°, and the higher complexity at 45° angle compared to 90° angle, emphasize the importance of selecting the right camera angle based on the specific task requirements and desired outcomes.

7 Limitations

The prototype and study presented in this research have several limitations that were necessary to ensure the accuracy and consistency of the data collected from all participants. However, these limitations restrict the generalizability and scope of the findings. The height at which the drone operated during both tasks was kept constant. This decision ensured that all participants interacted with the drone at the same vertical distance, eliminating any variability in data due to changes in height. Varying the height could have introduced differences in task difficulty and participant performance, making it challenging to attribute differences in results to the camera angles alone. The drone's movements were limited to forward and backward directions. This simplification was essential for obtaining accurate and comparable data from all participants. Allowing multi-directional movement could have introduced additional complexity and variability, potentially affecting the reliability of the results. By restricting the drone's movement, we ensured a controlled environment where the primary variable of interest camera angle could be accurately assessed. The weight of the package that the drone was required to pick up in the drone delivery task was kept constant. This control was crucial to ensure that the drone's stability and movement were not affected by variations in weight, which could have influenced the difficulty of the task and the performance of the participants. By maintaining a constant weight, we could better isolate the impact of camera angles on task performance.

8 Conclusions and Future Work

The study investigated the impact of three different camera angles 0°, 45°, and 90° on task performance, situation awareness and workload in two distinct scenarios: assembly line monitoring and drone delivery, inside a factory environment. The results and discussion lead to several important conclusions. The 45° camera angle consistently offered the best performance for the assembly line monitoring task, whereas the 90° camera angle performed the best in the drone delivery task. In the assembly line monitoring task, the 45° angle resulted in the shortest total time compared to the 0° and 90° angles. The number of errors detected was highest at the 45° angle compared to the 0° angle and 90° angle. This suggests that the 45° angle provided a more effective visual perspective for identifying errors while also allowing for faster completion times in assembly line monitoring tasks. In the drone delivery task, the 90° camera angle demonstrated superior performance overall. The total time for task completion was significantly lower at the 90° angle compared to 0° angle and 45° angle. Additionally, the pick-up time was shortest at the 90° angle, indicating greater efficiency in initial task execution. The drop-off times for the 45° and 90° angles were almost identical, showing that both angles facilitated quicker drop-offs. Moreover, the distance to the target was smallest at the 90° angle compared to 0° angle and 45° angle, demonstrating greater precision in drone navigation and control. These results indicate that the 90° angle provided a more effective visual perspective for the drone delivery task, allowing for more accurate and efficient performance.

For situation awareness in the assembly line monitoring task, the 90° angle had less instability and complexity compared to the 0° angle. The 45° angle had the highest complexity. In the drone delivery task, the 45° angle had higher complexity and the 90° angle had higher variability. These findings indicate that different camera angles impact the cognitive load associated with situational awareness, with the 90° angle generally resulting in less cognitive strain in the assembly line monitoring task but more variability in the drone delivery task.

Regarding workload, in the assembly line monitoring task, the 90° angle led to higher physical and mental demand as well as effort required. In contrast, the 45° angle had the lowest physical and mental demand, required less effort, and showed the highest performance. In the drone delivery task, the 90° angle had the lowest mental demand, the highest physical demand, the highest performance, and the lowest effort. The 0° angle resulted in the highest mental demand, lowest performance, highest effort, and highest frustration. These findings suggest that while the 90° angle can improve performance and precision, it also increases physical demands, whereas the 45° angle offers a better balance of workload demands in both tasks.

Future research should consider several extensions of this study. One important next step would be to explore the effects of varying drone heights and allowing multi-directional movements. This would provide a more comprehensive understanding of how these variables interact with camera angles to influence performance and workload. Additionally, investigating the impact of camera angles in more dynamic and complex environments could yield insights that are more applicable to real-world scenarios. Finally, examining how varying object weights affect drone stability and task performance could provide a deeper understanding of operational limits and capabilities under different conditions.

9 References and other appendices

[1] I. J. Akpan and O. F. Offodile, “The Role of Virtual Reality Simulation in Manufacturing in Industry 4.0,” *Systems*, vol. 12, no. 1, p. 26, Jan. 2024, doi: 10.3390/systems12010026. Available: https://www.mdpi.com/2079-8954/12/1/26.

[2] É. Beke, A. Bódi, T. G. Katalin, T. Kovács, D. Maros, and L. Gáspár, “The Role of Drones in Linking Industry 4.0 and ITS Ecosystems,” in *2018 IEEE 18th International Symposium on Computational Intelligence and Informatics (CINTI)*, Nov. 2018, pp. 000191–000198. doi: 10.1109/CINTI.2018.8928239. Available: https://ieeexplore.ieee.org/document/8928239.

[3] “A constructive heuristic for the heterogeneous drone delivery problem that considers packages’ setups and battery capac….” Available: http://ouci.dntb.gov.ua/en/works/7A0mRg39/.

[4] T. M. Fernández-Caramés, O. Blanco-Novoa, I. Froiz-Míguez, and P. Fraga-Lamas, “Towards an Autonomous Industry 4.0 Warehouse: A UAV and Blockchain-Based System for Inventory and Traceability Applications in Big Data-Driven Supply Chain Management,” *Sensors*, vol. 19, no. 10, p. 2394, Jan. 2019, doi: 10.3390/s19102394. Available: https://www.mdpi.com/1424-8220/19/10/2394.

[5] J. Czentye, J. Dóka, Á. Nagy, L. Toka, B. Sonkoly, and R. Szabó, “Controlling Drones from 5G Networks,” in *Proceedings of the ACM SIGCOMM 2018 Conference on Posters and Demos*, Budapest Hungary: ACM, Aug. 2018, pp. 120–122. doi: 10.1145/3234200.3234244. Available: https://dl.acm.org/doi/10.1145/3234200.3234244.

[6] K. Spanaki, E. Karafili, U. Sivarajah, S. Despoudi, and Z. Irani, “Artificial intelligence and food security: swarm intelligence of AgriTech drones for smart AgriFood operations,” *Production Planning & Control*, vol. 33, no. 16, pp. 1498–1516, Dec. 2022, doi: 10.1080/09537287.2021.1882688. Available: https://www.tandfonline.com/doi/full/10.1080/09537287.2021.1882688.

[7] “Drones in Manufacturing: A Game-Changer for Industry • Viper Drones,” *https://viper-drones.com/*. Available: https://viper-drones.com/industries/infrastructure-drone-use/manufacturing/.

[8] “Industrial Drone Inspection transforms industrial Operations.” Available: https://www.energy-robotics.com/post/how-industrial-drone-inspection-will-transform-the-future-of-efficient-operations.

[9] “The Benefit of Drones in the Construction Industry.” Available: https://www.commercialuavnews.com/the-benefit-of-drones-in-the-construction-industry.

[10] "Drones In Factory Surveillance and Monitoring • Viper Drones," *https://viper-drones.com/*. Available: https://viper-drones.com/industries/infrastructure-drone-use/drones-in-factory-surveillance-monitoring/.

[11] D. Mourtzis, J. Angelopoulos, and N. Panopoulos, "UAVs for Industrial Applications: Identifying Challenges and Opportunities from the Implementation Point of View," *Procedia Manufacturing*, vol. 55, pp. 183–190, Jan. 2021, doi: 10.1016/j.promfg.2021.10.026. Available: https://www.sciencedirect.com/science/article/pii/S2351978921002237.

[12] S. Awasthi, N. Gramse, D. C. Reining, and D. M. Roidl, "UAVs for Industries and Supply Chain Management," 2022, doi: 10.48550/arXiv.2212.03346. Available: http://arxiv.org/abs/2212.03346.

[13] O. Maghazei, T. H. Netland, D. Frauenberger, and T. Thalmann, "Automatic Drones for Factory Inspection: The Role of Virtual Simulation," in *Advances in Production Management Systems. Artificial Intelligence for Sustainable and Resilient Production Systems*, A. Dolgui, A. Bernard, D. Lemoine, G. von Cieminski, and D. Romero, Eds., Cham: Springer International Publishing, 2021, pp. 457–464. doi: 10.1007/978-3-030-85910-7_48

[14] A. Zenkin, I. Berman, K. Pachkouski, I. Pantiukhin, and V. Rzhevskiy, "Quadcopter Simulation Model for Research of Monitoring Tasks," in *2020 26th Conference of Open Innovations Association (FRUCT)*, Apr. 2020, pp. 449–457. doi: 10.23919/FRUCT48808.2020.9087391. Available: https://ieeexplore.ieee.org/document/9087391.

[15] C.-G. Oh, K. Lee, and M. Oh, "Integrating the First Person View and the Third Person View Using a Connected VR-MR System for Pilot Training," *Journal of Aviation/Aerospace Education & Research*, vol. 30, no. 1, pp. 21–40, Jan. 2021, doi: https://doi.org/10.15394/jaaer.2021.1851. Available: https://commons.erau.edu/jaaer/vol30/iss1/2

[16] https://unity.com/

[17] https://assetstore.unity.com/

[18] https://www.turbosquid.com/

[19] https://grabcad.com/

[20] https://www.blender.org/

[21] https://www.autodesk.com/products/3ds-max

[22] https://www.nvidia.com/omniverse

[23] L. Grip, *Vision based indoor object detection for a drone*. 2017. Available: https://urn.kb.se/resolve?urn=urn:nbn:se:kth:diva-208890.

[24] K.-H. Seok, Y. Kim, W. Son, and Y. S. Kim, “Using Visual Guides to Reduce Virtual Reality Sickness in First-Person Shooter Games: Correlation Analysis,” *JMIR Serious Games*, vol. 9, no. 3, p. e18020, Jul. 2021, doi: 10.2196/18020. Available: https://www.ncbi.nlm.nih.gov/pmc/articles/PMC8323020/.

[25] R. Shi, H.-N. Liang, Y. Wu, D. Yu, and W. Xu, “Virtual Reality Sickness Mitigation Methods: A Comparative Study in a Racing Game,” *Proc. ACM Comput. Graph. Interact. Tech.*, vol. 4, no. 1, p. 8:1-8:16, Apr. 2021, doi: 10.1145/3451255. Available: https://doi.org/10.1145/3451255.

[26] J. Won and Y. S. Kim, “A New Approach for Reducing Virtual Reality Sickness in Real Time: Design and Validation Study,” *JMIR Serious Games*, vol. 10, no. 3, p. e36397, Sep. 2022, doi: 10.2196/36397. Available: https://www.ncbi.nlm.nih.gov/pmc/articles/PMC9555332/.

[27] S. Ang and J. Quarles, “Reduction of cybersickness in head mounted displays use: A systematic review and taxonomy of current strategies,” *Front. Virtual Real.*, vol. 4, Mar. 2023, doi: 10.3389/frvir.2023.1027552. Available: https://www.frontiersin.org/journals/virtual-reality/articles/10.3389/frvir.2023.1027552/full.

[28] https://ww2.unipark.de/

[29] S. Masnadi, K. Pfeil, J.-V. T. Sera-Josef, and J. LaViola, “Effects of Field of View on Egocentric Distance Perception in Virtual Reality,” in *Proceedings of the 2022 CHI Conference on Human Factors in Computing Systems*, in CHI ’22. New York, NY, USA: Association for Computing Machinery, Apr. 2022, pp. 1–10. doi: 10.1145/3491102.3517548. Available: https://doi.org/10.1145/3491102.3517548.

[30] R. Temma, K. Takashima, K. Fujita, K. Sueda, and Y. Kitamura, “Third-Person Piloting: Increasing Situational Awareness using a Spatially Coupled Second Drone,” in *Proceedings of the 32nd Annual ACM Symposium on User Interface Software and Technology*, in UIST ’19. New York, NY, USA: Association for Computing Machinery, Oct. 2019, pp. 507–519. doi: 10.1145/3332165.3347953. Available: https://doi.org/10.1145/3332165.3347953.

[31] J. O. Wobbrock, L. Findlater, D. Gergle, and J. J. Higgins, “The aligned rank transform for nonparametric factorial analyses using only anova procedures,” in Proceedings of the SIGCHI Conference on Human Factors in Computing Systems, in CHI ’11. New York, NY, USA: Association for Computing Machinery, May 2011, pp. 143–146. doi: 10.1145/1978942.1978963. Available: https://doi.org/10.1145/1978942.1978963.

[32] M. Georgsson, “NASA RTLX as a Novel Assessment Tool for Determining Cognitive Load and User Acceptance of Expert and User-based Usability Evaluation Methods,” *European Journal of Biomedical Informatics*, 2020, Available: https://www.ejbi.org/abstract/nasa-rtlx-as-a-

novel-assessment-tool-for-determining-cognitive-load-and-user-acceptance-of-expert-and-userbased-usabilit-5988.html.

[33] “Situation Awareness Rating Technique (SART),” 2019. Available: https://www.semanticscholar.org/paper/Situation-Awareness-Rating-Technique-(SART)/c5a666e196248fa600aca27445ea6f00c7cbd85d.

List of Abbreviations

VR – Virtual Reality

IoT – Internet of Things

DT – Digital Twin

MR – Mixed Reality

UAV – Unmanned Ariel Vehicle

3D – 3 Dimensional

HMD – Head Mounted Display

CSV – Comma Separated Values

SART – Situation Awareness Rating Technique

NASA-RTLX – Raw NASA Task Load Index

SD – Standard Deviation

Declaration of Independence

I Declare that I have carried out and written this work independently. Sources, literature and tools used by me are marked as such.

Signature

Qasim Saboor